

Assessment of UV Index using artificial neural networks

By
Sep Human

Dissertation submitted in compliance with the requirements for Masters Degree in Technology in the Department of Electrical Engineering (Light Current) at Teknikon Natal.

This dissertation represents my own work

~~Sep Human~~

APPROVED FOR FINAL SUBMISSION

Professor Vladimir B. Bajic, D. Eng.Sc.(E.E.)
Supervisor
Deputy Head of the BioDiscovery Group,
Laboratories for Information Technology,
Singapore.
Professor Kevin Duffy PhD,
Co-Supervisor
Centre for Engineering Systems Research
Teknikon Natal

15/4/2002

Date

Contents

1	Introduction	10
1.1	South Africa, UVR and Health risk	10
1.2	Motivation	11
1.3	Data and Modelling	12
1.4	Research Goals and Scope	13
1.5	Potential Social Impact	14
2	UVR and Human Health	15
2.1	The Human Skin	15
2.2	The Eye	16
2.3	Protection	17
2.3.1	Sunscreens	17
2.3.2	Clothing and Hats	18
2.3.3	Sunglasses	18
2.3.4	General Protection	19
2.4	South African Situation	19
2.4.1	Concluding comments	23
3	Ultraviolet Radiation (UVR)	24
3.1	Some Terminology and Physical Dimensions	24
3.2	Radiation	25
3.2.1	UVR types	26
3.2.2	UVC Radiation	27

3.2.3	UVB Radiation	27
3.2.4	UVA Radiation	28
3.3	UVR Exposure	28
3.4	Measurement	29
4	The UVB Index	32
4.1	Dosimetry	33
4.1.1	UVI	35
4.2	Action Spectra	37
4.3	Forecasting the UVI for Durban	39
4.4	Global Solar UVI	41
4.5	UVI Maps	41
5	Solar Survey & Preliminary Analysis	43
5.1	Solar Survey	43
5.2	Data	45
5.2.1	Continuous and discrete variables	45
5.2.2	Categorical and fuzzy variables	45
5.3	Analysis by regression methods	48
5.4	Logistic Regression Results	50
6	UVI Models Based on ANNs	52
6.1	Data Preparation	52
6.2	Training of the First ANN Model	53
6.3	Results Obtained With the First ANN Model	56
6.4	Second ANN Model of UVI	58
6.5	Results for the Second Model	59
6.5.1	Reduction of data - a way to improve the model	61
6.6	Third Model	62
7	Conclusions	71

List of Figures

2-1	Sunshine hours in Durban vs. day in January 2000.	20
2-2	The distribution of the South African population according to languages.	21
4-1	The UVI during a typical South African sunshine day.	33
4-2	UVI at 272 different South African observation sites.	34
4-3	UVI at different times of the day at visited observation sites. The line connecting the points on the graph indicate the sequence of sites visited.	35
4-4	Burn time in min related to UVI categories.	36
4-5	Relative erythema effectiveness vs. UV wavelength.	38
4-6	Predicted UVI for Durban.	40
5-1	Cloud cover as assessed on specific dates.	46
6-1	Simplified presentation of an RBNN (Orr 1999).	54
6-2	Distribution of errors in % that RBNN model produces in estimating the UVI on the training set.	55
6-3	Distribution of cumulative errors in % that RBNN model produces in estimating the UVI on the training set.	56
6-4	Distribution of errors in % that RBNN model produces in estimating the UVI on the test set.	57
6-5	Distribution of cumulative errors in % that RBNN model produces in estimating the UVI on the test set.	58

6-6	Simplified structure of a three layered feed-forward neural network. In our case the output neurons are linear, while the hidden layer neurons are of 'tansig' type, thus having $h_j(x) = \frac{e^x - e^{-x}}{e^x + e^{-x}}$. The initial number of neurons in the hidden layer was 60, and through the pruning process it has been reduced so as that the prediction performance of the neural network model has improved.	60
6-7	Distribution of prediction errors in the training set with the improved model.	61
6-8	Distribution of prediction errors in the test set with the improved model.	62
6-9	Distribution of cumulative prediction errors in the training set with the second model.	63
6-10	Distribution of cumulative prediction errors in the test set with the second model.	64
6-11	Distribution of prediction errors in the first reduced training set with the second model.	65
6-12	Distribution of prediction errors in the first reduced test set with the second model.	65
6-13	Distribution of cumulative prediction errors in the first reduced training set with the improved model.	66
6-14	Distribution of cumulative prediction errors in the first reduced test set with the improved model.	66
6-15	Distribution of prediction errors in the second reduced training set with the second model.	67
6-16	Distribution of prediction errors in the second reduced test set with the second model.	67
6-17	Distribution of cumulative prediction errors in the second reduced training set with the improved model.	68

6-18 Distribution of cumulative prediction errors in the second reduced
test set with the improved model. 68

6-19 Distribution of predictive errors on the test set for the third model. . 69

6-20 Cumulative error distribution for the third model on the test set given
in %. 70

List of Tables

2.1	Skin types according to FDA.	16
2.2	Skin cancer diagnosed in South Africans (Sitas 1998)	22
3.1	Type of UVR by wavelength ranges	26
6.1	UVI for a sample of locations in South Africa	54
6.2	Number of data if different clusters	59

Dedication

I dedicate this dissertation to my four daughters Anso, Liesl, Carin and Corné. May their mental neural networking make them efficient and as a result, happy **humans**.

Acknowledgement

My sincere thanks and appreciation are extended to the following:

- The Lord for His guidance in my life and for enabling me to complete this study.
- Professor Vladimir B. Bajic, Deputy Head of the BioDiscovery Group, Laboratories for Information Technology, Singapore) for his friendship, supervision, and priceless academic support.
- Dr. Pavel Tabakov for his valued and timesaving assistance when editing this dissertation.
- Ron Hacking for his typically colonial type comments and help whilst proof-reading drafts of this thesis.

Chapter 1

Introduction

1.1 South Africa, UVR and Health risk

South Africa is a country with a variety of climatic regions and topological diversity. The country ranges from the sub-tropical East Coast, through the summer rainfall highveld (>5000 feet) to the very arid and desert-like West Coast with hardly any vegetation. The Cape Town area, called the Western Province, again, is a winter rainfall region. The doses of ultraviolet (UV) radiation (UVR) in South Africa can change significantly depending on the location and other factors like cloud cover, etc.

With regards to UVR, South African region bears many similarities to Australia. The Southernmost town in South Africa, Cape Agulhas (34°S, 19°E), is on about the same latitude as Perth and Sydney in Australia. UV indices greater than 10 (they are in the range from 0 to 15) are common in South Africa, and this is similar to Australian conditions. In South Africa, the number of sunshine hours per day, as well as the ambient UVR levels, are high throughout the year. South Africa has one of the highest levels of UVR in the world.

The UV Index (UVI) (see WHO/EHG 1999) provides a measure of the UV irradiance on the ground. The UVI includes biological criteria (Diffey 1998) which incorporate the way in which different human skin types absorb UV energies. Some

relevant aspects of solar energy absorption enter complicated domains of dermal photobiology and photochemistry (see Holick 2000).

The UVI is considered extremely important when gauging doses of solar UVR absorbed by humans. Since the absorbed doses of UVR are cumulative (Slaney 1998), it may happen that an individual has absorbed too much of it, which ultimately may cause different health problems (see CIE 1987, Gies 1998). Generally, exposure to sunlight, a fair skin, and high levels of UVR increase the potential health risk. These include skin cancer, serious damage to the immune system, and eye disorders, even blindness due to cataracts as a result of long term damage to the human eye (see, for example, Gies 1997, Mackie 2000, Diffey and Gies 1998, Gies et al 1998).

Because of the reasons mentioned above, it is not strange that South Africa has a high incidence of skin cancer (Sitas et al 1998) and eye disorders in the human population. Skin cancer occurrences for South Africans, Australians and Zimbabweans are amongst the highest worldwide. With this in mind, and having essentially high risk UVR situations throughout the year in the whole South Africa, it is in the interest of public health to provide information to the population on the possible UV irradiation and associated health risks.

1.2 Motivation

This research is motivated by the need to factually inform the local population and tourists on solar UVR they may be exposed to. The South African Weather Bureau does not yet (September 2001) forecast the numerical values of the UVI. Thus, currently, no such specific information is provided for the general public in South Africa.

Most first-world countries have sophisticated, integrated, fully automated, and extremely expensive, systems and networks that provide media with weather and UVI forecasts (see, for example, Long 1997). Due to the present state of the South African economy, it is not likely that such systems will be implemented in South Africa in the near future. Consequently there is scope for development of much more

affordable UVI forecasting systems.

This research project aims at developing the basic elements of such a system. Its goal is to enable modelling of UVI for the whole of the South African territory. The UVI models should provide sufficiently accurate UVI assessment at any site in South Africa, subject to the condition that the relevant parameters at these sites are known. These parameters should be obtainable by means of relatively cheap systems/equipment, so that it is possible to establish a network that will cover South Africa.

1.3 Data and Modelling

To assure the feasibility of such a project, we had to collect the relevant data from different South African locations. This data was not available until recently. To cover the vast geographic area of South Africa, a survey was conducted in January 1999, providing the raw data used in these analyses. The Centre for Engineering Research (CER) at Technikon Natal, Durban, was the first to record ultraviolet irradiances on the ground in South Africa as a whole (Bajic and Human 1999). This survey covered a comprehensive number of sites throughout the country and resulted in a database containing data for 272 sites. This data was used in developing and testing the UVI prediction models (Bajic and Human 1999, Human and Bajic 2000).

The data collected included estimated and categorical variables. The categorical variables were cloud cover, albedo, turbidity and terrain, and they were estimated. The problem was to develop a model for inferring the level of UV irradiance from imprecise measurements/data collected. Techniques based on regression methods were attempted, but failed to produce satisfactory results. The problem to infer the UV index value from the data appeared to be a complex one. We finally resorted to the utilization of ANN for resolving this problem (Bajic and Human 1999, Human and Bajic 2000). This approach proved to be extremely successful.

In this project new concepts and completely new technology in developing the UVI model are used, as opposed to the CART regression approach utilized by Bur-

rows (1997). Because of the fuzzyness and imprecision of some of the categorical data (such as albedo, cloud cover, terrain and turbidity) (Viertl 1996) used in the description of the different sites, the regression techniques failed to produce sufficiently accurate models. Neural networks based modelling of the UVI, however, produced sufficient accuracy in excess of 88% (see also Human and Bajic 2000, Human 2000). These results are excellent, if compared with those produced by very costly and elaborate countrywide networks such as those in use in Canada (Long 1997). The results obtained in this research are acceptable, but can be improved given more sophisticated equipment, time and funding. The investigation is directed at minimizing undesirable health effects to the South African population, and to allow them to enjoy outdoor activities more safely in the long term.

1.4 Research Goals and Scope

This research is based on the following.

- **Hypothesis.** It is possible to infer the UVI value based on the data that include assessments/measurements of time, latitude, longitude, altitude, temperature, humidity, cloud cover, turbidity, albedo and terrain.
- **Assumptions.** 1/ The values associated with the categorical variables (cloud cover, turbidity, albedo and terrain) defined them properly and with sufficient precision. 2/ The model obtained from this data will result in sufficient accuracy of UVI predictions.
- **Problem definition.** Develop a model for inferring the UVI level based on variables including imprecise and fuzzy ones contained in the dataset collected during the South African solar survey in January 1999 (Bajic and Human 1999).
- **Delimitations.** This research project will not develop a commercial system for UVI predictions.

1.5 Potential Social Impact

Our efforts at researching and modelling the UVI in South Africa was predicated in the fact that understanding, and being able to predict the intensities of UVR, would ultimately make significant changes to our UV awareness and the health and well-being of the entire UVR educated population. UVR in sufficient doses, sunlight exposure, and skin cancers, are correlated and irreversibly related as shown from years of research (Diffey 1998). It is **impossible** to increase public understanding of the harmful effects of UVR and to propagate the necessity of changes in our interaction with the sun, without having a daily UVI forecast, at least one day in advance. These values must be distributed nationally by the news and electronic media. For the same reason all educational and awareness campaigns relating to skin cancer should be based on understanding the UVI, as it is a direct measure of solar UV irradiance. Note that many South Africans are encountering high doses of UVR as an occupational hazard (farmers and outdoor workers). By making larger segments of the South African population aware of the health risks associated with the high UVR will reduce the number of health problems extensively, and subsequently also reduce the associated very high specialized medical costs. Additional benefit could be the reduction of the absenteeism which will impact positively on the GNP of South Africa.

The outcome of our entire modelling exercise is aimed at the younger portion of the target population, i.e. school children. Firstly educating this sector of the population will definitely help us achieve our goal of establishing a population core of UVR educated South Africans, sooner.

Chapter 2

UVR and Human Health

In this chapter we will present some of the basic facts about the influence of sunshine (UV portion of the electromagnetic spectrum of the sun) to human health, as well as some comments on the South African situation in this regard.

2.1 The Human Skin

The skin serves as a protective layer of the body and it also regulates body temperature. Skin types are classified into several groups regarding their sensitivity to UVR (Summers 1999). Different skin-types respond differently to UVR. Naturally the skin acts as a barrier to UVR and has unique repair systems depending on the skin type (Summers 1999). The American Food and Drug Administration (FDA) lists the human skin into six categories (see Table 2.1)

Damage to the human body due to UVR is cumulative and reduces the efficiency of the immune system (Holick 2000). Mutation of DNA caused by this UVR may be followed by tumor promotion (Norval 2000). Currently, the mechanisms that lead to cancer development as a consequence of DNA damage caused by UVR, is not fully understood. Further investigation into photobiology, photochemistry and re-

Skin type	Response	Characteristics
I	always burns easily never tans	redheads; freckled Celtic
II	burns easily tans minimally	fair-skinned; fair-haired Caucasians
III	burns moderately tans gradually	darker Caucasians
IV	burns minimally always tans well	Latins Arabs
V	rarely burns tans profusely	Asians Negroids
VI	burns very slightly on longer exposure; deeply pigmented	Negroids

Table 2.1: Skin types according to FDA.

radiation (by bodycovering suntan lotions - see Summers 1999) may provide answers on the progression of normal skin cells to cancerous ones.

2.2 The Eye

Chronic exposure to high levels of solar radiation contributes to the age-related macular degeneration of the retina, a major cause of blindness. Some 20 million people worldwide are currently blind as a result of cataracts. The World Health Organization estimates that 20% of these people are blind due to UV exposure (WHO 1999). Direct viewing of the sun and other bright objects may so seriously impair vision that any task that requires recognition of fine details, such as sewing and reading, will be made impossible. Experts believe that each 1% sustained decrease in atmospheric ozone would result in an increase of 0.5% in the number of cataracts caused by solar UVR (Diffey Erythema Spectrum 1999).

Solar eclipses are viewed by many people. The necessity to protect the human eye while observing this phenomenon is usually overlooked. Retinal injuries and even loss of eyesight may result. Cases of defective eyesight are underreported as patients consult eye specialists long after viewing an eclipse (Sliney 1998). "Eclipse blindness" is not generally associated with having looked at the sun for only a few

seconds. Although the sun is 150 million kilometers away, the sensation of warmth (infrared radiation) is experienced when sunlight shines on our skin. The eye acts as a convex lens and concentrates the light on the retina such that it burns the cells of the retina, when viewing the sun directly, even only for a very short time. The cells become damaged irreversibly and that part of the retina induces local blindness (WHO 1999). Thus, it is not advisable to use sunglasses, exposed film or smoked glass, to look directly at the sun. Only filters (marked as #10 or #12) used by welders (exposed to actinic radiation) should be used as they provide sufficient UV protection. The use of unmarked filters is not recommended at all (Mellerio 1998).

2.3 Protection

If the surface area of the human body exposed to UVR is large and or if the UV exposure time is extended, for reasons of safety the shielding aspect becomes very important (Gies 1999). Sensible reduction of UV doses can be affected by simply keeping out of the sun between the hours of, say, 9h00 to 15h00 (Fig. 4-1). The cloud cover, as well as smoke, reduce clear-sky UVR by up to 50% (Burrows 1997). If the occupational situation requires work outdoors, then protection takes on a different meaning (Gies 1992). Sunscreens and appropriate clothing, hats and sunglasses, make up part of the gear (ARPANSA 1999) to be worn in order to be safe (Gies 1994, 1997), when active outdoors (Osterwalder 2000). Shadecloth of different densities (Moon 1995) provides another means of protection, especially with the very high UVR during the summer months in South Africa (van Tonder 1998).

2.3.1 Sunscreens

Cosmetics cannot offer complete protection against UVR. Though shade may reduce UVR by 50%, diffuse sunlight can still do damage, even underneath an umbrella. It is therefore wise to have several means of protection. Sunscreens must be used together with clothing, hats and sunglasses. Broad spectrum sunscreens protect

against UVA and UVB (for explanation of UBA and UVB see Chapter 4) and must be applied in preference to those types offering protection against UVB only (Diffey 1989).

Some cosmetic products have the Sun Protection Factor (SPF) indicated. SPF tells us what kind of protection we are getting when applying such products. SPF 20, if applied generously, halves the risk if compared with SPF 10 sunscreen, with the same duration of exposure. It, however, does **not** imply (Cesarini J. P. 2000) that if the SPF is doubled, say from SPF 15 to SPF 30, that you can double exposure time.

2.3.2 Clothing and Hats

Textiles are rated similarly to sunscreens. The protection factor in this case however is called an Ultraviolet Protection Factor (UPF) (Hilfiker 1989). If a textile is certified to have an UPF of more than 50, that implies that the textile provides an excellent UVR protection (Lowe 1995). Swing tags generally identify not only the rating organization or laboratory that tested the materials in question, but also the UPF (Menter 1994). Good protection is rendered by textiles with a rating of UPF 15 and higher (Diffey 1992).

2.3.3 Sunglasses

Eye UVR exposure risks may be reduced if hats are combined with a good pair of sunglasses for protection purposes. Lenses should block out at least 95% of UVR. Wraparound sunglasses should be checked for fit both on the brows and temples as these give almost complete protection only if they fit properly. Plane (flat) lenses are subject to the Coroneo effect and some 5% of ambient UVR (the so-called obliquely incident, i.e. reflected from the rear surface of the lens) still reaches the eyes. Sunglass lenses are rated regarding the UVR protection it renders with an EPF (Eye Protection Factor).

Optochromic, polaroid and silvered lenses do not, as frequently believed, absorb

UVR completely. When selecting sunglasses one must ensure that the % UVR transmission is low (up to 5%). Children especially should have parental guidance in this selection and sunglasses should primarily be effective in filtering harmful UVR and should not only be a fashion item. Diffuse UVR, as a result of reflection, especially off fresh clean snow (where 80% UVR is reflected) and beach sand (where this reflection is 25%) makes sunglasses a necessity if a person is exposed to such conditions. Snow-blindness is a known problem with snowboarders and skiers if these precautions are overlooked.

2.3.4 General Protection

Oil crises had a negative effect on the automotive industry, when fuel prices simply soared. This in turn resulted in sleeker designs, with the percentage glazing on vehicles increased. This is done to reduce the coefficient of friction in order to combat the high fuel consumptions. More glazing on vehicles possibly increases transmitted UVR and doses to vehicle occupants. Therefore, Gies (1992) suggests that UPFs for clear and tinted windscreens had to be researched.

In the medical field, although hightech and professional techniques are involved, these do not result in complete safety for patients at all times. For example, dentists nowadays use UVR to cure synthetic fillings in teeth. Many of these collimated UVR sources are not of the "piped" types and scattering of the UVR delivers high doses to gums (IRPA/INIRIC 1989). Also, ophthalmologists use lasers, some of which produce UVR, to perform delicate operations on human eyes (Lowe and O'Hagan 2000). Standards for ophthalmic instruments are not yet completely implemented and adhered to by surgeons (Slaney 1987, 1998).

2.4 South African Situation

South Africa is blessed with good sunny weather. As an example, the mean number of **sunshine hours** in Durban (at a latitude $29^{\circ}S$ and longitude $30^{\circ}E$) during

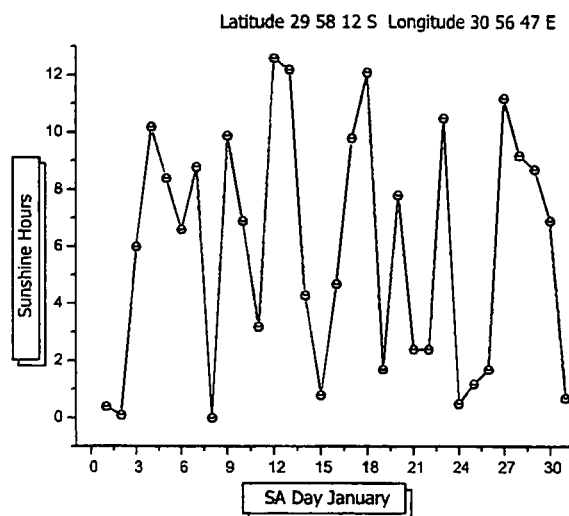


Figure 2-1: Sunshine hours in Durban vs. day in January 2000.

January 2000, was 6.15 h, including a maximum of 12.6 h during the same month (see Fig. 2-1)(SAWB 2000). The maximum *UVI* reading for the same month, recorded by the Centre for Engineering Research, was 15 (Human 2000). In contrast, in some regions in Europe and the Northern Hemisphere it is possible to have as little as 12 h of sunshine for the entire month!

Our ultimate goal of UVR awareness in South Africa is to enable South Africans to change their attitudes towards the sun so that they may be able to enjoy the outdoors safely through knowledge of the potentially harmful aspects of UVR. Personal sun safety will also benefit if there is an understanding of the interaction of the sun and skin, and if the public is educated in that respect.

Given the heterogeneity of the South African population (more than 40 million), and considering the diversity of languages and literacy, we begin to understand that this goal represents a formidable task (see Fig. 2-2). The South African population consists mainly of Black, Colored, Indian and White people. The variety of skin pigments and their different UV absorptive natures generates complex and mostly

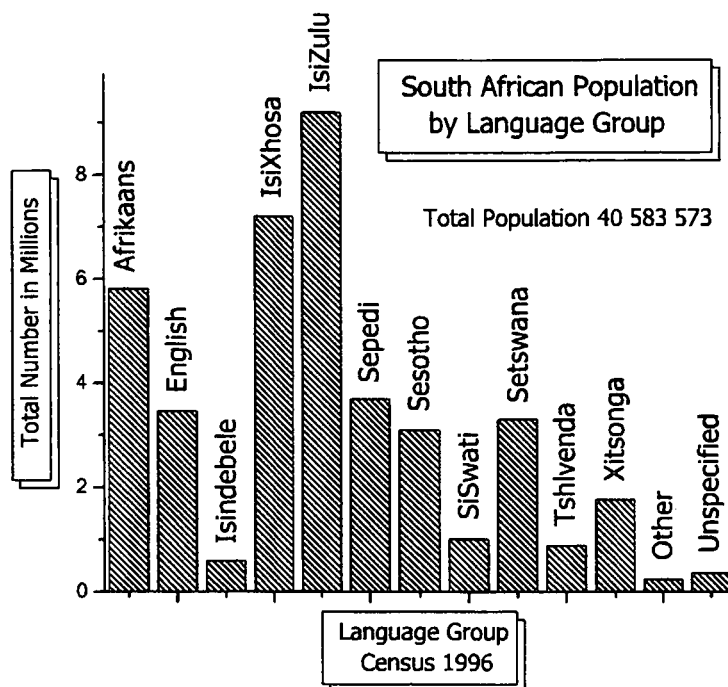


Figure 2-2: The distribution of the South African population according to languages.

unknown problems within the realms of photobiology and photochemistry.

For the reasons of significant illiteracy and language diversity in South Africa one realizes just how absolutely necessary it is to eliminate such concepts as "burn time" and to introduce a simple yet effective means of communicating UV irradiance and UV dose to the South African public, and especially to children (Moise 1999).

When looking at histologically diagnosed skin cancer cases in South Africa, and if we consider the main population groups, the statistics are truly alarming (NRPB 1995 - see Table 2.2). This entire research project is directed at being able to model, assess, and predict the UVI anywhere in South Africa. **As the UVI is then known beforehand**, and the public is aware of the potential risks, then long-term benefits (Sinclair 2000) will be experienced in South Africa (Cesarini 1998). This will not only

Race	Sex	Basal and squamous cell cancer	Malignant melanoma	Total
Asian	Males	25	5	30
	Females	10	3	13
Black	Males	364	85	449
	Females	328	131	459
Colored	Males	49	3	52
	Females	44	11	55
White	Males	5884	398	6282
	Females	3946	401	4347
TOTAL		10650	1296	11946

Table 2.2: Skin cancer diagnosed in South Africans (Sitas 1998)

reduce the number of skin cancer cases, but the GNP will increase as the very high medical costs associated with skin cancer and cataracts will be reduced substantially. For example, during September 2000, the Centre for Engineering Research (CER) at the Technikon Natal, Durban, as part of an applicable and educational community service, issued a flyer —“**SAFE UVI INFO**” not only classifying four skin types, but also relating the precautions to be taken based on the categories of the UVI. These precautions clearly outlined when to apply sunscreens, when to wear hats, and UV efficient sunglasses.

The UVR exposed surface area of the human body should be considered a serious contributor to severe sunburn, a condition that should be avoided at all cost. In a country as sunny as South Africa most of us are reluctant to sensibly utilize textiles (long pants, long sleeved shirts and hats) and good sunglasses to reduce UV dose and lasting damage to ourselves. This, however, remains one of the best ways to safeguard one's health, in the long run, since by practising them the absorbed doses are significantly reduced, and one need not recourse to sunscreens or other forms of protection. Being in the shade of a tree can reduce the *UVI* by as much as 50%. Reduction of the UV dose can therefore be effectively taken care of in this simple, but practical, way without having to employ elaborate equipment to establish doses, etc. It should be kept in mind that about 60% of UV dose is received between 09h00 and 15h00 and that no daylight saving is practised in South Africa. South Africans

should change their behavior to reduce doses of UVR, yet to still be outdoors a lot and to be able to enjoy the sun **safely**. Sensible and simple precautions include:

- **Cover up** – with comfortable clothing to keep the sun off your skin (Stanford 1995). Wear a longsleeved shirt and a hat, preferably with a wide brim and UV efficient wraparound sunglasses (Gies 1990, Diffey 1992).
- **Protect children**. Blistering sunburn during childhood can lead to skin cancer in later life. Keep babies (less than 3 months old) out of the sun completely.
- **Seek shade** – especially during the hottest part of the day, from 9h00 – 15h00. Shade can reduce UV by 50% or more (Toomey 1995).
- **Take care NOT to burn** – sunburn increases your risk of skin cancer.

2.4.1 Concluding comments

Although the awareness drive and the educational aspects about harmful effects and the risks involved in UV exposure will be expensive and slow, it **MUST** be brought to the attention of the entire population, especially young children. Only now, after twenty years, the Australian "SunSmart" programme is showing positive results. Such perseverance and continued expenditure by the Australian government is surely commendable. For a project of this nature to succeed it will need sound administration and will require long term support of the government of the day. Only then there will be chances of success. Awareness drives, through focussed educational programmes followed by dissemination to the general public and specifically schoolchildren, produces an understanding and appreciation of the UVI. The precautions based on the UVI could be used nationally for sunsafe outdoor behavior by the population. The proposed South African project, like the Australian "SunSmart" programme, will have to be a long term one before any benefits and improvements will accrue to the skin cancer situation (Sinclair 2000).

Chapter 3

Ultraviolet Radiation (UVR)

In this chapter we will present some background of the UVR and, where appropriate, relate these to health problems.

3.1 Some Terminology and Physical Dimensions

In this present work only solar radiation is considered. In describing an irradiated surface, like the human body, one needs additional concepts, such as energy, power, radiance and irradiance.

In photobiology, photochemistry and the physics of irradiated surfaces the following quantities are in use:

- **Irradiance** (or surface dose **rate**) specifies the power incident on a plane. Its unit is $W \times cm^{-2}$
- **Radiant exposure** (or surface **dose**) is the energy incident on a plane. Its unit is $J \times cm^{-2}$.
- **Fluence** represents the portion of the solar energy density absorbed by body and it includes internal backscatter. Its unit is $J \times cm^{-2}$.
- **Fluence rate** (fluence/time) in human skin tissue (concerns multiple scattering events within the derma). It is commonly confused with irradiance. Its

unit is $W \times cm^{-2}$.

- **Radiant intensity** is power per steradian and specifies the source and degree of collimation. Its unit is $W \times sr^{-1}$.
- **Radiance** is solar power density. It is used when dealing with retinal hazards. Its dimension is $W \times cm^{-2} \times sr^{-1}$.
- Spectral quantities per wavelength range (such as UVB, UVA) are used when quoting energy, power or irradiance per wavelength interval. When calculating a photo-biologically effective dose, the spectral quantity must be multiplied by the corresponding (constant) entry in the action spectrum for the specified wavelength interval to obtain the spectral power density in $W \times cm^{-2} \times nm^{-1}$.

3.2 Radiation

The radiation known to us as UVR ranges from 290 nm to 400 nm in the electromagnetic spectrum. We should at all times distinguish between the effects of visible light (400 nm – 700 nm) and UVR (Webb 2000). Ionizing radiation, nonionizing radiation, and doses of UVR, are governed by factors such as distance from the source, time of exposure, and shielding from the radiation. As we are considering UVR in particular, taking the sun to be the only UVR source, this makes distance negligible (distance of earth from sun is approximately $150 \times 10^6 km$). The effects of UVR exposure time and shielding on skin will hinge on dosage, exposure duration and what kind of precautions should then be taken. Generally, over 90% of UVR can penetrate light cloud. Clean snow reflects up to 80% of sunburning UVR, whereas sand reflects up to 25%. UVR increases by 4% for each 300 m increase in altitude. Up to 60% of UVR is received between 10h00 and 14h00 daily. Shade can reduce UVR by up to 50%. Indoor workers receive 10% to 20% of outdoor worker's yearly UV exposure. UVR is 40% as intense at 0.5 m below water level, as on the surface (ARPANSA 2000).

Type of UVR	wavelength range
UVC	200nm-290nm
UVB	290nm-320nm
UVA1	320nm-360nm
UVA2	360nm-400nm

Table 3.1: Type of UVR by wavelength ranges

3.2.1 UVR types

UVR penetrates the human skin as easily as X-radiation passes through the human body. Terrestrial sunlight contains UVR, besides visible and infrared radiation. The spectrum of UVR includes three different wavelength ranges denoted as UVC, UVB and UVA (Table 3.1). Sunlight reaching the ground normally consists of UVR with wavelengths between 290 and 400 nm and visible radiation with wavelengths from 400 to 780 nm (Kok 1979). The UVR spectrum considered ranges from 290 nm to 400 nm (DeLuisi 1998).

Fortunately, UVC does not reach sea level, as it completely absorbed from sunlight by absorption and scattering in the atmosphere of the earth. Scattering is inversely proportional to wavelength to the fourth power. The shorter the wavelength, however, the higher the energy and therefore the greater the potential for damage to the human body. The longer the wavelength of the UVR, the deeper the penetration into the skin.

If we evaluate in electron-volts the energy of one photon related to UVA1, with a wavelength of 320 nm, then

$$E = h\nu,$$

$$\lambda = \frac{c}{\nu},$$

$$\begin{aligned} E &= \frac{hc}{\lambda} \\ &= (6.6 \times 10^{-34} \times 3 \times 10^8) / (320 \times 10^{-9}) \text{ J} \\ &= (6.6 \times 10^{-17} \times 3) / (320 \times 1.6 \times 10^{-19}) \text{ eV} \\ &= 3.87 \text{ eV}. \end{aligned}$$

This is the maximum UVR energy that is theoretically carried by one photon that can be transferred from the photon to the human body for a wavelength of 320 nm.

3.2.2 UVC Radiation

UVC is very noxious to DNA. Fortunately it is not of any danger in reality. Ozone absorbs UVC in the upper atmosphere and UVR of these wavelengths only reaches the peaks of very high mountains, such as Muona Lua, Hawaii, peaks in the Alps, etc. Unfortunately, ozone depletion also takes place, which increases the danger of UV exposure. Ozone is depleted mainly because of the presence of chloro-fluoro carbons (CFCs) as generated in industry and as in aerosols. Developing countries will be using CFCs for another 10 years at least, which amounts to about 10,000 tons per year (McCulloch 1997).

3.2.3 UVB Radiation

Energy from the sun arrives as a mix of UV, visible, infrared energy and cosmic radiation. About 34% of this energy is reflected back into space before reaching the surface of the earth. UVR energy in the wavelength range 290 nm–320 nm (i.e. UVB) is sufficient to damage DNA and can destroy DNA molecular bonds. It

reduces the immunity of the human body. Erythema or reddening of the skin, heat, blistering and peeling, and other discomforts are caused by excessive exposure to UVB.

Looking at the human erythema action spectrum, and the relative response shown for UVB, suggests why UVR of this wavelength range plays a major role in causing skin cancer (de Gruijl 2000). Chronic and accumulative excessive exposure to UVB, ultimately causes melanoma and non-melanoma cancers (Jonker 1994). Abandonment of the precautions implied by the level of *UVI*, will certainly see an increase in skin cancer cases in the long term.

3.2.4 UVA Radiation

The longer wavelength UVA penetrates the human skin deeper than UVB despite transferring less energy. UVA quickly tans or darkens the human skin because it changes the melanocytes within the surface layers of the skin. After prolonged exposure, UVA is still harmful and causes ageing, the loss of resilience and fragility of the skin (NRPB 1995).

A distinct need for obtaining the maximum value of the UVA radiation levels in the world and South Africa has recently arisen because of the relatively new broad spectrum sun lotions that are manufactured (Summers 1999). These sunscreens need to maximize the absorptive qualities of the UVR attenuating agents. The lotions will then have the added advantage over ordinary UVB lotion types by being broader spectrum lotions and able to counteract some of the harmful UVA effects as well.

3.3 UVR Exposure

The absorbed UV energy is accumulative (Sasaki 1998). This implies that the absorbed UVR dose and its possible harmful effects would not be nullified if the person, after such exposures, refrained from any further exposure to sunlight. Severe

blistering during childhood, due to sunburn, is directly related to development of skin cancer in later life (Moise 1999). The risk of developing skin cancer may be reduced by as much as 50%, if:

- UV protective care is applied from an early childhood (O'Riordan 2000), and
- provided the UV doses are limited as far as is practically possible until the age of 18 years (Gies 1998).

Research (Holick 2000, Cullen 1998) **unquestionably relates skin cancers to UV exposure and overexposure**, but very interesting questions still remain unanswered:

- Are children exposed to UVR at a bigger risk than adults despite the much smaller surface areas of their bodies? (Gies 1998).
- Sunscreens, an interposed absorbant layer, re-radiate energy (Wilkinson 1998). Is this re-radiated energy harmful and different to UVR? (Dransfield 2000).
- Broad spectrum sunscreens: do they protect sufficiently well against photoaging and skin cancer?
- Skin cancer: is it the result of severe blistering sunburn during childhood on some occasions, or is malignant melanoma the result of cumulative lifetime exposure? (Diffey 1998). Experts are of the opinion that if proper UVR care is taken during childhood, then this will substantially reduce the probability of contracting skin cancer in later life.
- Sunbeds: UVR exposure and sources are well controlled in Scandinavia (Wester 2000). Are these sunbeds generally safe? (Hawk 2000).

3.4 Measurement

Depletion of stratospheric ozone increases the possibility of getting skin cancers. Attempts to combat skin cancers from this point of view emphasize the need for

selecting the most suitable data which could be used in addressing the issue of such a threat to human health. Measurements (Roy 1997), equipment, equipment calibration and the global intercomparisons of such apparatus, has to be coordinated for the data to be meaningful and, to some degree, uniformity has to be established (Rengarajan 2000). Unfortunately, such is the variation in terminology and units used, that data produced by scientists all over the world is nonstandardized. The need for global uniformity in this respect definitely exists.

Spectroradiometric measurements made in Pretoria (in Southern Hemisphere) during 1964–65 on daylight data (295–775 nm) yielded values for UVR and the blue regions of the sunlight spectrum that were considerably higher than those reported for the Northern Hemisphere. As measurements were made at an altitude of 1400 m, the CIE (Commission Internationale de l'Eclairage) unfortunately did not accept these results. Wavelengths below 400 nm were doubted by CIE and it was agreed that further measurements had to be furnished. Consequently another measurement programme was undertaken at sea level in Durban during the period of April 1976 to July 1977 (Kok 1979).

Dosimetry in skin photobiology, and the dynamics of photochemistry, require some means of measuring and quantifying UVR. The minimal erythral dose is called the *MED*. The basic unit for dose is defined by

$$1 \text{ MED} = \rho \text{ J m}^{-2},$$

and it represents the minimum dose for a type II skin (see Table 2.1) to show a beginning of reddening (erythema). The constant ρ , which appears in the above mentioned formula for the *MED* unit may differ for different countries (this is also a source of global non-uniformity). The *MED* cannot thus be taken as a standard. It is affected by many variables such as the ambient illumination, the anatomical site, skin pigmentation, time of observation after exposure, and dose increments. This may ultimately result in the use of the standard erythral dose, the *SED* (see later). Confusing and incorrect use of the term resulted in a suggestion that the

MED only be used for studies in humans and other animals. Biometers (such as Solar Light model 501) give the effective dose per hour or the irradiance (power per area) in *MED h*⁻¹.

$$\begin{aligned} 1 \text{ } MED \text{ } h^{-1} &= 250 \text{ } J \text{ } m^{-2} \text{ } h^{-1} \\ &= 0.0694 \text{ } W \text{ } m^{-2} \\ &= 69.4 \text{ } mW \text{ } m^{-2}. \end{aligned}$$

This really indicates that the time in hours to get sunburnt is the reciprocal of the irradiance in *MED h*⁻¹. For example, if UV irradiance is given as 2 *MED h*⁻¹, then the safe exposure time is obtained by reciprocating it, i.e. as 0.5 *h* = 30 minutes.

A standardized measure of erythemogenic UVR is the standard erythema dose (*SED*). One *SED* is equivalent to an erythema effective radiant exposure of 100 *J m*⁻² and is a measure of sunburning radiation. The unacclimatized skin of someone who always burns and never tans (see Table 2.1) would require an exposure of 1.5 *SED*, whereas a person who tans easily and rarely burns would need 6.0 *SED* to cause minimum erythema (Diffey 2000).

Chapter 4

The UVB Index

Skin cancer triggers the question on how to relate solar electromagnetic radiation (UVR within a certain wavelength bandwidth) and effective UVR dose received by the surface of the human body (NRPB 1995). Amidst all the complexities in the processes of absorbing solar energy, such as photobiology, photochemistry and radiation physics, we must consider a suitable unit of UV dose.

The UVI quantifies the effective UV dose. The UVI is a physical quantity. It is dimensionless, i.e. it is purely numerical; it ranges from 0 to more than 20. In our case we only dealt with the UVR in the wavelength range 290 nm to 320 nm, i.e. with the UVB (Bajic and Human 1999). A suitable action spectrum, the " Human Erythema Action Spectrum " was applied to derive the effective UVB dose. Thus we will talk about the UVB Index henceforth as the UVI. The UVI, a biologically-weighted (CIE 1987) physical parameter, will serve as a measure of the irradiance on the ground, and safety precautions will be based on its numerical value.

The UVI daily covers a range of values at one site. Therefore it does not indicate the maximum value only, at that site. This index changes abruptly with the cloud cover changing. Also, the maximum value recorded for any day does not necessarily coincide with 12h00 (midday) (Fig. 4-1). The graph in Fig. 4-1, is obtained by measuring the UVI at different times of the day and at different locations in the South African solar survey (Human 2000) (see Fig. 4-2, Fig. 4-3. It can be observed

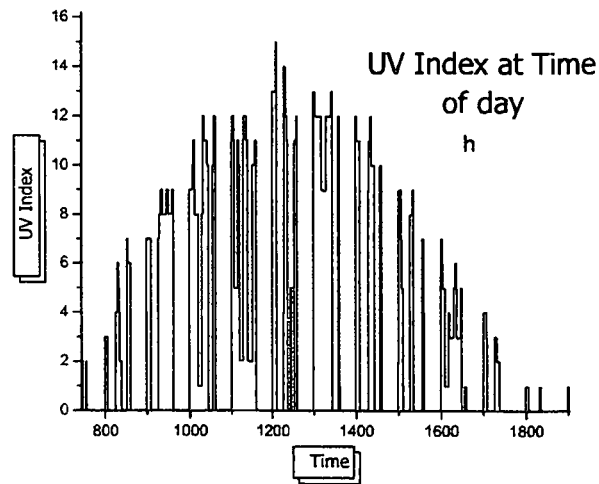


Figure 4-1: The UVI during a typical South African sunshine day.

that the UVI is dangerously high from as early as 09h00. Thus the maximum values of UVI, UVI_{\max} , must generally be associated with a time interval around 12h00 midday. These measurements were obtained by successively visiting different locations in South Africa (see Chapter 5 for route details).

4.1 Dosimetry

It must be pointed out that estimated UVI values as are available off the very latest (2001) UVI maps (see later) collected by satellites are clear sky readings and do not include haze and cloud cover. UVB irradiance on the ground, however, depends heavily on changes in cloud cover. Meteorological networks may therefore provide relevant and regional information that may not be sufficiently accurate. During our South African survey, the actual or true UV irradiance was measured on the ground which means that we included both the regular and diffuse UVR in all observations. All our readings incorporated variables such as albedo, cloud

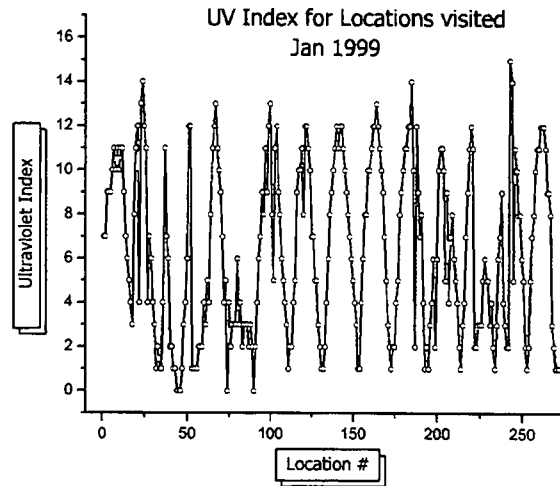


Figure 4-2: UVI at 272 different South African observation sites.

cover, terrain and turbidity, whose values are imprecise by nature. UVI maps do not include such specific and refined details. As will be seen later, these details helped us to develop very accurate models for the UVI assessment anywhere in South Africa. Naturally, our data also includes inaccuracies due to equipment calibration, etc., but the advantages of having the actual UVI at a particular location on the ground, outweighs these aspects, completely. The action spectrum applied during our survey to compute the effective dose, is that due to the CIE (Diffey and McKinlay 1987).

The interpretation of UVR dose as the allowed permitted sunburn time confuses the public since different erythral reaction times obviously exist for the different skin types. This is illustrated in Fig. 4-4, where the burn time relates to the numerical value of the UVI. The non-linearity shown by the exponential fit implies the complexity of such a relationship. Skin sensitivity to UVR varies extensively. In order to differentiate factually between different skin types, skin factors which relate to specific threshold erythral doses for each different skin type are expressed in both *MEDs* and Jm^{-2} per skin type. For example, a skin factor of 10 means

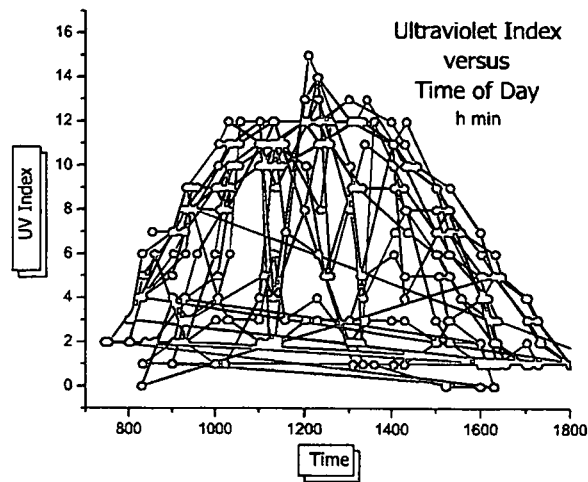


Figure 4-3: UVI at different times of the day at visited observation sites. The line connecting the points on the graph indicate the sequence of sites visited.

that skin type I person (see Table 2.1) will have a threshold dose of $1.51 \text{ MED} = 317 \text{ J m}^{-2}$. A skin factor 20 type person (rarely burns in sun) in turn will have a threshold dose of $11.91 \text{ MED} = 2500 \text{ J m}^{-2}$. This nonlinear relationship is obvious from Fig. 4-4. The US Environmental Protection Agency (EPA) has developed a skin classification scheme. Skin factors are correspondingly assigned for each elected skin category. A personal dosimeter manufactured by Safesun employs such specific standards where dosimetry depends on specific threshold doses analogous to skin type. The above facts obviously remove all thumbsucking from typical exposure and dose assessments. Equipment employing such standards if properly calibrated thus enables personal dosimetry in reality.

4.1.1 UVI

The *UVI* is defined with reference to a horizontal surface; it is biologically-weighted (CIE action spectrum) and it could be expressed numerically by multiplying the

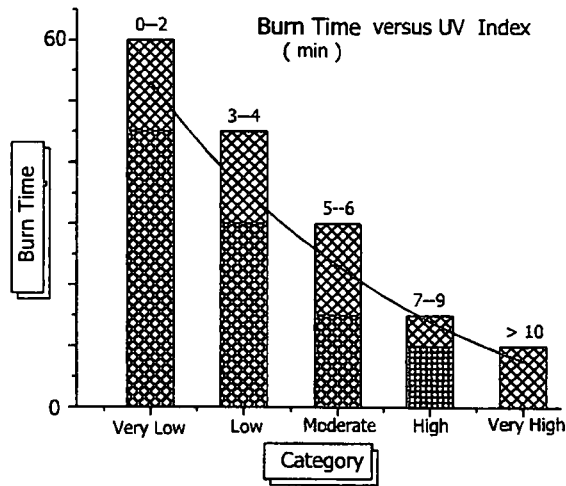


Figure 4-4: Burn time in min related to UVI categories.

effective irradiance (in $W m^{-2}$) by an appropriate factor. For example, in 1996, the CIE used the following definition of 1 *UVI*

$$\begin{aligned}
 1 \text{ UVI} &= \frac{1}{40} W m^{-2} \\
 &= 25 mW m^{-2}.
 \end{aligned}$$

Effective UVB means that the power of every wavelength incident (in the range 290–320 nm) on the human body, is multiplied by a coefficient (depending on the specific wavelength - see Fig. 4-5). These spectral coefficients relate to the sensitivity of the human skin for that wavelength. Integrating the effective power per wavelength across the entire UVB spectrum, gives the total effective irradiance. It should be kept in mind (see Chapter 3) that the *MED* specifies the minimum dose which gives a visible reddening of type II skin (burns easily, tans minimally - see Table 2.1). Utilizing the above mentioned definition of 1 *UVI*, one can relate *MED*

and the *UVI* in the following way:

If

$$1 \text{ MED} = 210 \text{ J m}^{-2} \text{ h}^{-1},$$

then

$$\begin{aligned} 6.24 \text{ MED} &= 6.24 \times 210 \text{ J m}^{-2} \text{ h}^{-1} \\ &= \frac{6.24 \times 210}{3600} \text{ W m}^{-2} \\ &= 0.36 \text{ W m}^{-2} \\ &= 0.36 \times 40 \text{ UVI} \\ &= 14.56 \text{ UVI} \end{aligned}$$

Thus $6.24 \text{ MED} = 14.56 \text{ UVI}$. The above interpretation is presently not valid in all countries actively involved in Global Atmospheric Watch (GAW) programmes any more. Several variations of the *UVI* are therefore in use.

4.2 Action Spectra

Less than 1% of solar radiation is in the UVB portion of the electromagnetic spectrum (290–320 nm). However, if the threshold for the type of skin exposed is exceeded long enough, reddening will occur (de Gruijl 2000). Sunburn is not directly proportional to the UV energy absorbed, but depends on the wavelength of the UVR. Skin type determines the sensitivity to UVR, but relative sensitivities to the wavelengths within the range considered, remain unaltered.

Action spectra describe the related effectiveness, at different wavelengths, of producing a specific biological reaction in, say, plants and humans (NASA). Such spectra provide the weighting for the UV spectrum, so that one can determine the total effective dose (D_{eff}) for sunburn. The mathematical expression for D_{eff} is

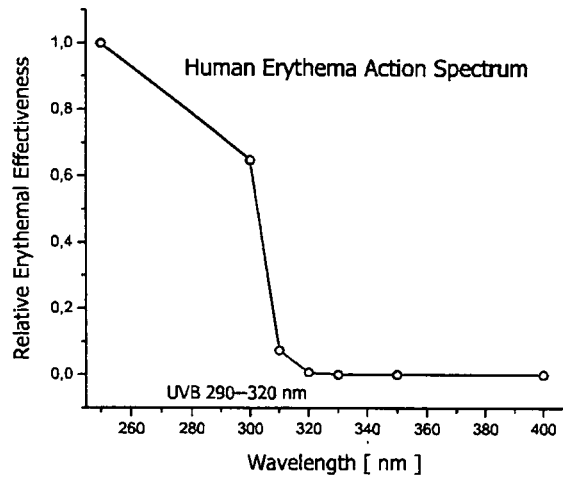


Figure 4-5: Relative erythema effectiveness vs. UV wavelength.

$$D_{eff} = \int_{290}^{400} I(\lambda)_{UV} \times A(\lambda) d\lambda,$$

where I_{UV} is the intensity of UVR, A is the coefficient from the action spectrum for the corresponding wavelength λ .

For example, Fig. 4-5 shows the dependence of relative erythema effectiveness on the UVR wavelength. We see a quick decline in the relative effectiveness as the wavelength increases. The UVB (290 nm – 320 nm) obviously is more effective than the UVA at causing the biological responses (such as severing DNA chains and reducing human immunity). Ozone depletion causes an increase in UVB levels, which in turn will be more severely harmful to human beings (Cesarini 1998b).

The consideration of the UVB effects should however not detract from realizing the importance of UVA (320–400 nm) and its contribution to harmful effects on the human body (Marks 1993). It will be a worthwhile project to repeat our survey in South Africa, this time recording UVA levels, and in doing so to establish the

maximum value UVA_{\max} for UVA in South Africa. Eventually, this could prove very helpful information in producing even more effective broad spectrum sunscreens.

The Reference Action Spectrum (RAS) by the CIE has almost universally been used since 1987. Several action spectra do however exist, for example for DNA damage, for non-melanoma skin cancers, for fish-melanoma, etc. Presently, the CIE is in the process of publishing the Risk Action Spectrum (RAS), which includes development of so-called "threshold limit values" (TLVs) for each type of skin that will provide means for setting standards for health protection. The cosmetic industry in turn needs RAS for "UV- induced human skin aging", "UV-induced delayed Pigmentation of human skin" and " Immediate Pigment Darkening". Research and work on these topics are in progress worldwide.

4.3 Forecasting the UVI for Durban

For the first time ever in South Africa, the UVI was predicted a day in advance for Durban on specific days during September 2000 (Cesarini P. 2000). The Centre for Engineering Research (CER) at Technikon Natal, Durban, deliberately selected those days to coincide with the Research Day held at this institution. The coordinates, determined by global positioning system using four satellites, were:

Latitude 29°58'12" S

Longitude 30°57'06" E

The UVI was 8 on September 12; 7 on September 13; then dropped to 5 on September 14, because of the cloud cover of 50% – 75%. During the modelling of the UVI, cloud cover was one of categorical and fuzzy variables. The cloud cover on day September 14, 2000, was specified as category 4 (see Chapter 5 and graphical profile in Fig. 4-6). A survey that was conducted by NASA using a total ozone mapping spectrometer (TOMS), relating the UVI and cloud cover for South Africa (January 1989) obviously depicted the same relationship as that shown in our Fig. 4-6.

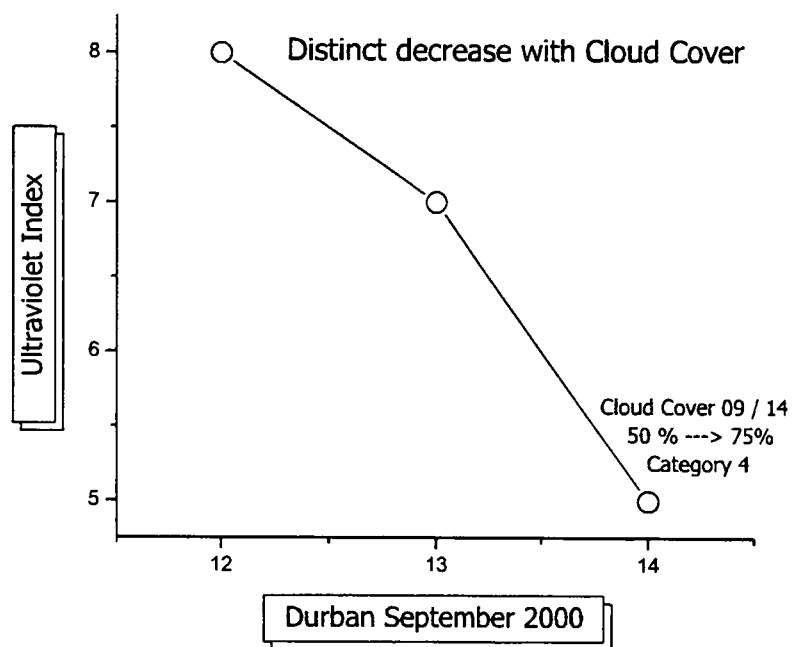


Figure 4-6: Predicted UVI for Durban.

4.4 Global Solar UVI

The World Health Organization (WHO) propagates the use of a uniform and universal UVI. This Global Solar UVI is to be used to avoid confusion as several other UV indices are in use all over the world. Many of these non-standardised indices are used commercially by sunscreen and cosmetics manufacturers and certainly cause more confusion.

International organizations such as the World Meteorological Organization (WMO), the United Nations Environment Programme (UNEP) and the International Commission on Non-Ionizing Radiation Protection (ICNIRP) all recommend that (WHO FACT SHEET 1999):

- the Global Solar UVI be used to raise public awareness of potentially harmful UVR, and to help the population to take the necessary precaution;
- national governments should be encouraged to sponsor educational programmes to combat skin cancer using this uniform solar UVI;
- all media should carry **only** the Global Solar UVI.

4.5 UVI Maps

Ozone depletion and increased terrestrial UVR are linked. Ecosystems are affected by this invisible UVR. Readily available and on-line UV data has become a need for a variety of users and for many different purposes, one of which is health protection. UV climatology and trends are absolute necessities in epidemiology and such health related programmes.

Low and high resolution UVI maps are derived from satellite measurements and these provide a lot of useful data. Several organizations emerged that cater for an everincreasing number of needs and end users of this data. Agriculture, more so now than ever before, makes use of sophisticated facts to increase production and to cope with problems of a weather related nature. Several groups acquire UV

facts from remote servers, located all over the world. The UVI databases are updated daily. Such databases are used to compose and colourkey UV maps, giving the clear-sky UVI, which are accessible via the Internet. Clear sky UVI estimates using Earth Probe/TOMS ozone data are then derived, but cloud cover is excluded. World UVI maps are provided by the Socioeconomic Data and Applications Center (SEDAC). The Center for International Earth Science Information Network (CIESIN) at Columbia University, has been designated by NASA to operate and maintain SEDAC.

American UVI maps are provided by the National Oceanic and Atmospheric Administration (NOAA) and the Environmental Protection Agency (EPA). The evaluation of the UVI generally does not include albedo, aerosols (atmospheric pollutants) or haze.

UVI maps for Australia and New Zealand are also available. Australian UVI forecasts are given for noon the following day. Forecasting the UV irradiance at ground level considers variables such as time, date, latitude, cloud, haze and ozone concentrations. The Commonwealth Bureau of Meteorology Australia, worked in conjunction with the Cooperative Research Centre for Southern Hemisphere Meteorology to develop a global computer model which is used to deduce the UV intensity anywhere in Australia after some necessary inputs are predicted. Cloudfree skies are again assumed. The information on this can be obtained from <http://www.safesun.com.au>.

MAUVE (mapping of UVR by Europe) is an organization which has been busy establishing data maps on UV surface radiation and is supported by the European Commission (EUC) in the 4th R&D Framework Programme. A choice of products could eventually satisfy the demands by customers (Peeters 2000).

Although still part of an expensive service and lacking the accuracies required, such UVI maps will be the answer to South African needs. Not only could it supply a vast and varying land with the regional UVI, but forecasts can be made available daily, free to all, via the electronic and other media.

Chapter 5

Solar Survey & Preliminary Analysis

In this chapter we describe the solar survey conducted in South Africa, data collected in this survey, and the applied standard regression modelling of the UVI.

5.1 Solar Survey

To be able to cover the vast geographic area of South Africa a survey was conducted in January 1999, providing the raw data used for modelling the UVI. We attempted to infer the level of UV irradiance from measurements/data collected. The most important variables in modelling the UVI are:

- zenith angle,
- cloud cover,
- albedo,
- precipitation (rain), and
- haze.

During our survey albedo, cloud cover, terrain and turbidity were used. The zenith angle was not recorded during the survey. Terrain and turbidity were used instead of precipitation and haze. Data, consisting of some 10 continuous and discrete variables, were collected on the ground, throughout South Africa, at locations with widely varying terrain characteristics, e.g. from popular beaches to high altitude arid areas. The survey commenced on January the 14th, 1999, in Durban. It then followed the coastline down to Cape Town, up the West Coast to Springbok, then across to the East Coast via Pretoria and Komatipoort to end up back in Durban on the 29th of January, 1999.

This survey was conducted during January 1999 in order to compare the results with some UVR results from NASA that were available for this same month. These results of biologically active UVR, were derived at the earth's surface using a total ozone mapping spectrometer (TOMS) to measure total ozone abundance (Lubin 1998). UVR surface flux was obtained from the Earth Radiation Budget Experiment (ERBE).

January is mid-summer and a popular holiday period in the Southern Hemisphere. During this period many people spend time outdoors and are exposed, frequently overexposed, to UVR, especially on the beaches. The irradiance, captured as the UVI, was treated as the dependent variable within each of the attempts to model the UVI (Bajic and Human 2000, Human 2000). It was later determined that some independent variables were sensitive to the degree of sophistication of the UVI model, but it was decided to keep these imprecise or assessed variables part of the model equations.

The survey started in Durban at latitude $29^{\circ} 58' 12''$, longitude $30^{\circ} 57' 06''$ on January the 14th at 8h54. The route covered 272 locations, including places such as Port Elizabeth, Knysna, Hotazel, Upington, Nelspruit, Mbabane, Richards Bay and Mkuze. The maximum distance, 888km was covered on the 16th of January, with the last data collected at Qunu (location #31) at 16h39. For example, at one observation location the following data were collected:

Latitude 31° 46' 49"
Longitude 28° 37' 11"
Altitude: 930 m (3040 feet)
Temperature: 33.2 ° C
Humidity: 58%
UVI: 3
Cloud Cover: 0% → 25%
Turbidity: ≤ 7 km
Albedo: Green grassland (UVB diffuse reflectance 0.8% → 1.6%)
Terrain: Level and small village.

5.2 Data

5.2.1 Continuous and discrete variables

A list of continuous and discrete variables, as treated by multiple linear regression analysis, is as follows:

Y is **UVI** considered as the dependent variable
 X_1 is the **serial #** of the location (or code of the location)
 X_2 is **time** in hours and minutes
 X_3 is **latitude** in deg min seconds
 X_4 is **longitude** in deg min seconds
 X_5 is **altitude** in feet
 X_6 is **temperature** in °C
 X_7 is **humidity** in %.

5.2.2 Categorical and fuzzy variables

The following categorical variables have finite values and they were subjectively assessed:

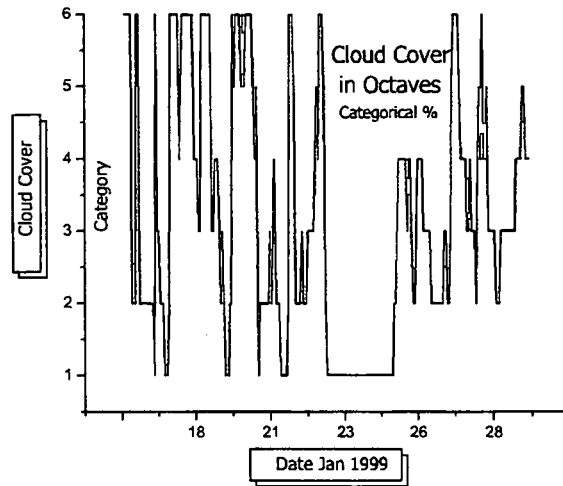


Figure 5-1: Cloud cover as assessed on specific dates.

X_8 relates to **Cloud Cover** given in %; its ranges were

$X_8 = 1$ for 0% cloud cover

$X_8 = 2$ for $0\% < \text{cloud cover} < 25\%$

$X_8 = 3$ for $25\% \leq \text{cloud cover} < 50\%$

$X_8 = 4$ for $50\% \leq \text{cloud cover} < 75\%$

$X_8 = 5$ for $75\% \leq \text{cloud cover} < 100\%$

$X_8 = 6$ for 100% cloud cover

See Fig. 5-1 for Cloud Cover during the survey.

X_9 represented **Turbidity** (visible 400 – 700 nm wavelength range);

its ranges were taken as the visibility measured in km:

1 for $0 \leq \text{turbidity} < 0.5$

2 for $0.5 \leq \text{turbidity} < 1$

3 for $1 \leq \text{turbidity} < 3$

4 for $3 \leq \text{turbidity} < 5$

5 for $5 \leq \text{turbidity} \leq 7$.

X_{10} represented **Albedo**; its ranges were adopted as:

1 for green grassland

2 for dry and arid soil

3 for wooden deck/dock

4 for black asphalt

5 for concrete

6 for dry beach sand

7 for wet beach sand

8 for sea foam

X_{11} represented **Terrain**; its assigned values were:

1 for flat/level terrain

2 for hilly terrain

3 for mountainous terrain

4 for open terrain

5 for suburban terrain

6 for urban terrain.

5.3 Analysis by regression methods

Preliminary attempts to develop a model for UVI assessment using multiple linear regression failed because:

- not all the variables were continuous, and
- some contained finitely few possible values.

This technique resulted in only 31% of the overall explained variation in data, suggesting the need to improve the model.

As a remedy, the range of the dependent variable of the study was subdivided into two parts in an attempt to create a dichotomous dependent variable. The derived new variable Y dependent on UVI was assigned the following values:

$$Y = \begin{cases} 1 & \text{when } UVI \geq 8 \\ 0 & \text{when } UVI < 8 \end{cases}.$$

Again the percentage of correct classification was small.

Since the use of linear regression failed to produce a good model, the logistic regression analysis was attempted. It appeared that further dichotomization will have to be implemented, but this would be a daunting task as many possible choices could be assigned to the categorical variables. Owing to the nature and diversity of some of the categories of fuzzy data (imprecise variables such as eg. albedo) it proved impossible to form logically similar "groups" when assigning 1 and 0 to these data clusters. Variable X_8 , listed above, gives an idea of just how different the categories to which 0 was assigned really are. These inputs, combining continuous and categorical variables, generated unacceptable coefficients in the earlier models relating the UVI to $Y = G(X_2, X_3, \dots, X_{11})$.

The categorical variables (cloud cover, terrain, albedo and turbidity) and the UVI were this time dichotomized. The logistic regression of Y on the 10 explanatory variables was then performed.

The list of variables and the chosen values were as follows:

The dependent variable of the model in this case remains that same as previously given:

$$Y = \begin{cases} 1 & \text{when } UVI \geq 8 \\ 0 & \text{when } UVI < 8 \end{cases}$$

The following 10 independent variables were used:

X_2 to X_7 as given previously. The other four were fuzzy in nature and categorical and this time they were assigned the following values:

$$X_8 = \begin{cases} 1 & \text{when cloud cover} < 25\% \\ 0 & \text{when cloud cover} \geq 25\% \end{cases}$$

$$X_9 = \begin{cases} 1 & \text{when } 0 \leq \text{turbidity} < 1 \\ 0 & \text{when } 1 \leq \text{turbidity} \leq 7 \end{cases}$$

$$X_{10} = \begin{cases} 1 & \text{on dry beach sand and barren soil} \\ 0 & \text{on green grassland, wooden deck/dock, black asphalt,} \\ & \text{concrete, wet beach sand, sea foam} \end{cases}$$

$$X_{11} = \begin{cases} 1 & \text{when terrain is flat/level or open} \\ 0 & \text{when terrain is hilly, mountainous, suburban, or urban} \end{cases}$$

In this variable selection we have five dichotomous variables: Y , X_8 to X_{11} . Each dichotomous variable has assigned two values: high and low (1 denotes one value, while 0 denotes another value). Because Y is dichotomized, we can think of it as representing a probability that when $Y = 1$ that will mean that the UVI will be high (and therefore dangerous to be exposed to UVR since then $UVI \geq 8$). Also, one can think of the four independent dichotomized variables as contributing significantly to this probability when they attain the high value.

The logistic regression of Y on the variables X_2 to X_{11} was then performed. The stepwise backward elimination procedure was used to identify factors that strongly affect the UVI. At each stage of the analysis, the backward elimination procedure discards the least important variable from the logistic regression model. The process of elimination stops when no more "useless" variables can be removed from the model. The model obtained at the end of the backward elimination procedure is called the "optimum logistic regression model" (Rosner 1990) and was used to interpret the results.

5.4 Logistic Regression Results

The logistic regression model relates to the probability of the $UVI \geq 8$, as

$$P(Y = 1) = \frac{1}{1 + e^{-Z}},$$

where Z is estimated through the above-mentioned procedure of backward elimination as:

$$\begin{aligned} Z = & 2.5341 - 0.74 \times \text{Albedo} - 0.0003 \times \text{Altitude} \\ & - 1.1608 \times \text{CloudCover} - 0.000018 \times \text{Latitude} \\ & - 0.0020 \times \text{Time} + 6.85 \times \text{Turbidity}. \end{aligned}$$

Using the above equations, one can estimate the **probability that $Y = 1$** (i.e. that $UVI \geq 8$) for any given set of values of the variables included in the formula. In other words if, anywhere in South Africa, these variables are known, then the probability of the UVI being greater than or equal to 8 units can be determined (i.e. the UV irradiance is dangerously high).

The percentage of correct classification for the model quoted is 73% and this shows that the estimated logistic regression model performs reasonably well and that it is reliable for the available data. One can notice that the backward elimination procedure retained six variables as the most representative for assessment of the UVI. Three of these six variables are fuzzy by nature.

Let β denote any estimated regression coefficient in the above formula for Z . Let $\exp \beta$ represent the odds ratio. In the case of turbidity $\beta = 6.8545$, which gives $\exp \beta = 948.1379$. This indicates that the turbidity is generating an anomaly in the model, since $\exp \beta$ is about one thousand times larger than the corresponding values for the other variables which should be of the order of one.

It was therefore decided to make use of artificial neural networks (ANNs), in order to accommodate difficulties introduced by these imprecise (fuzzy) variables.

Chapter 6

UVI Models Based on ANNs

As shown in the previous chapter, attempts at modelling UVI using linear and nonlinear regression from the data gathered in the South African survey from 1999, failed to produce acceptable results. The reason is because of the variety of choices when dichotomizing the categorical and fuzzy data. That problem led to the use of artificial neural networks (ANNs) to model the UVI (see Bajic and Human 1999, Human and Bajic 2000).

Regression techniques require independence between variables. This means that the variables are treated as not influencing one another. Regression coefficients do not take into account the interaction between two or more variables. ANNs do not require the same independence. For this reason, one can expect that models generated by ANNs may be sometimes much more accurate than models obtained by other techniques. For the references on ANNs see for example Zurada (1992).

6.1 Data Preparation

The purpose of the survey conducted in January 1999 was to record and assess a specific set of data (ten variables, including several estimated and categorical ones) and to infer the UV Index based on survey data. In total, data were collected for 272 locations. Coordinates of some of the locations visited are given in Table 6.1. The

following variables were considered: latitude, longitude, time, humidity, ambient temperature, cloud cover, albedo, turbidity and terrain, as listed in the previous chapter. The last four were estimated and categorical.

For example, at location number 243, a UV index of 15 was measured on the 28th of January at 12h 09min. The altitude was 4500ft (1371m) and the coordinates were of Mnyokane (Swaziland), 26° S, 31° E. Cloud cover was 50% to less than 75%. The ambient temperature was 32.4° C and the geography was mountainous with reflective eroded cuttings (roadworks). Under a nearby tree the UV index had a range of 3 (max 4 and min 1) (Weihs 2000).

The raw survey data was first normalized, because the data was represented in different scales and units. After normalization each input variable had a standard deviation of 1 and zero mean value. The normalization of the output data (the UVI) is also normalized in the same fashion.

After normalization, the original data set is divided into two subsets, the training set and the test set. This data separation was based on a random choice of sites to be included in each of the sets. We elected to have the training set data from 174 locations, and the test set data from 98 locations.

6.2 Training of the First ANN Model

Our goal was to infer the value of *UVI* expressed as *Y* from the collected data expressed by X_1 to X_{11} . The variable X_1 which represents the serial number of the observation site, was excluded from consideration since it does not contribute any information to the UVI value. Consequently we had only 10 independent variables X_2 to X_{11} .

The model should conform to the expression

$$y = G(x_2, \dots, x_{11}),$$

where y, x_2, \dots, x_{11} denote the normalized values of the original variables Y, X_2, \dots, X_{11} ,

Location	Latitude	Longitude	Time	UV Index
	° ' "	° ' "	h min	
Durban	29 58 12	30 57 06	9 53	8
Port Alfred	33 35 29	26 53 52	9 00	1
Port Elizabeth	33 58 16	25 37 49	10 34	6
Jeffreys Bay	34 02 04	24 55 48	12 01	7
Knysna	34 04 45	23 03 44	8 32	4
Mossel Bay	34 10 59	22 08 54	12 31	13
Cape Agulhas	34 49 59	19 59 50	8 38	2
Cape Town	33 53 26	18 29 08	16 07	5
Springbok	29 39 59	17 53 00	9 45	8
Upington	28 27 32	21 14 37	17 36	2
Hotazel	27 43 24	23 04 14	10 32	10
Pretoria	25 51 27	28 10 19	11 02	11
Mbabane	26 22 59	31 09 55	12 58	5
Hluhluwe	28 01 17	32 16 12	10 57	12
Richards Bay	28 41 48	32 00 43	12 54	11

Table 6.1: UVI for a sample of locations in South Africa

respectively. The ANN has to be constructed so that its nonlinear transfer function can sufficiently well approximate the above mentioned relationship. Although there are many possible choices for the structure of ANNs and for the methods of their training (see Zurada 1992), we selected a radial basis neural network (RBNN) (Orr 1999) to generate the UVI prediction model (see Fig. 6-1).

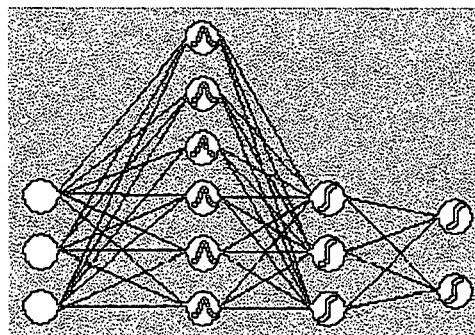


Figure 6-1: Simplified presentation of an RBNN (Orr 1999).

The RBNN was trained on the data from the training set. The RBNN has a

number of tunable parameters. One of these is the bias of the radial basis functions. For different values of that parameter, different approximation quality of the RBNN are achieved. The selection of the best values of the biases is not trivial and is data dependent. Another problem is the complexity of the RBNN, i.e. how many neurons the RBNN should have. Determining the optimal number of neurons is also a non-trivial problem (Orr 1999).

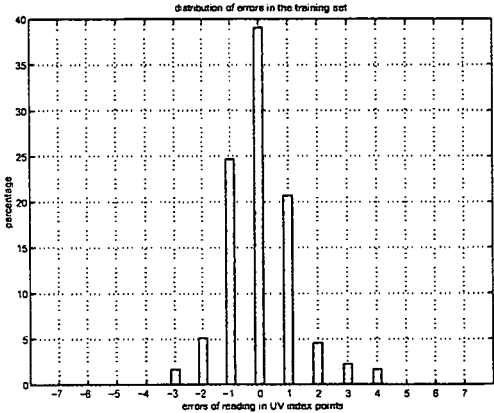


Figure 6-2: Distribution of errors in % that RBNN model produces in estimating the UVI on the training set.

We used a tri-fold cross-validation procedure for determining the parameters of the RBNN. This means that we divided the training set (by random choice of the observation sites) into three non-overlapping subsets of 58 observation sites in each of them. Then, the data from any two of these subsets were used to train the RBNN for the best results on the remaining third subset. This procedure was repeated numerous times in an optimization process (based on simplex method - see Nelder and Mead 1965) which determined, in addition to the standard weights of the RBNN, also the optimal values for the number of neurons in the network and the optimal values for the bias of the radial bases functions.

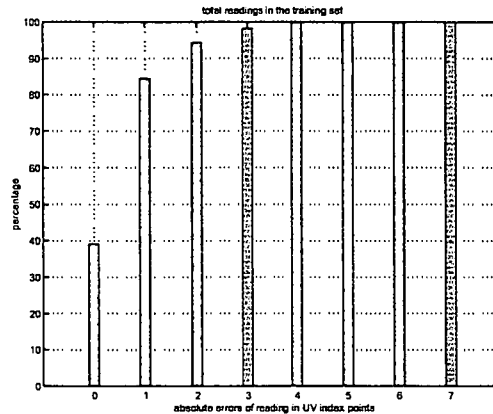


Figure 6-3: Distribution of cumulative errors in % that RBNN model produces in estimating the UVI on the training set.

6.3 Results Obtained With the First ANN Model

The trained network has produced very interesting results. These are summarized in distributions depicted in Fig. 6-2 to Fig. 6-5. Fig. 6-2 and Fig. 6-4 show the normalized distributions of the error of the UVI estimates that RBNN model makes relative to the target UVI values. Cumulative estimates of the UV index relative to errors are depicted in Fig. 6-3 and Fig. 6-5.

The behavior on the training set was very good. For example, in about 40% of cases there was zero error in predicted values of the UVI. Also, in 25% of cases in the training set the estimated value of the UV index was with an error of -1 (i.e. if the UV index was estimated at 11, its actual value was 12). Even better indication of the good behavior of the model is that in about 95% of cases in the training set, the maximal error of estimation was ± 2 as can be seen from the distribution graph of cumulative errors (i.e. if the estimated value was 10, the actual value could be anything from 8 to 12). These observation imply that, at least on the training set, the model was quite good.

However, although the behavior of the model on the training set is good, it is

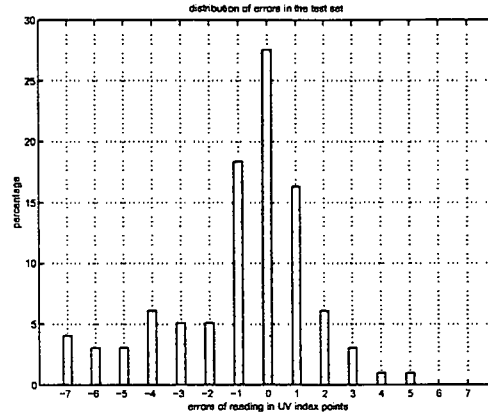


Figure 6-4: Distribution of errors in % that RBNN model produces in estimating the UVI on the test set.

not an indication that the model will behave well on the test set. The real test of the ability of the model to correctly predict the UVI has to be assessed on the test set data. One should note that the ANN model of the UVI was not exposed to the data contained in the test set before the test. So, by using the data from the test set the model is faced with the completely new data and, if it is a good model i.e. if it can generalize well, it would be able to produce reasonable values of the UVI. The results on the test set are depicted in Fig. 6-4 and Fig. 6-5.

The results for the test set, as can be seen from the relevant figures are not as good as on the training set. This can be seen from both of the graphs that relate to it. However, this is what one can expect. The reasons are that, firstly, that the available data set is relatively small, and secondly, the imprecision of some of the basic input data does cause the problems similarly as was the case in the regression modelling in the previous chapter. With a more complete data set one could expect that the model may improve significantly. However, although the model behavior on the test set is not as good as on the training set, the model is able to predict the UVI with the maximal error of ± 4 in 88% of cases. Note that with the same maximal prediction error, the logistic regression model from the previous chapter

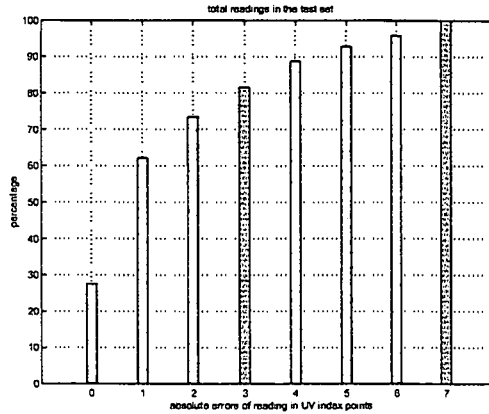


Figure 6-5: Distribution of cumulative errors in % that RBNN model produces in estimating the UVI on the test set.

correctly classified only 73% of data on the whole data set (in our case that would be both training and test sets).

6.4 Second ANN Model of UVI

In the previous section we applied the RBNN to model the UVI and the success was considerable as compared to the logistic regression modelling. However, since the data gathered during the South African survey was collected at various sites, some of which possessed certain similarities caused, in part, by the use of fuzzy variables, we suspected that possibly there are some natural clusters in the dataset. For this reason we attempted to use these potential clusters to improve the UVI model.

To cluster the data we used a Self-Organizing Map (SOM) ANN. The SOM ANN was trained in 200,000 epochs on the training set data, and grouped it into three clusters. For each of the clusters, an ANN was trained to make an assessment of the UVI from the data within the cluster. Table 6.2 shows the number of input-target data in each of the clusters.

	training set	test set
# of data	66	34
# of data	35	24
# of data	73	40

Table 6.2: Number of data if different clusters

The clustered data was normalized to the zero mean and standard deviation of 1. Then for each of the clusters in the training set the following procedure is applied. A feedforward three layered neural network (one hidden layer) with 'tansig' transfer neurons in the hidden layer and the linear neuron in the output layer was trained and pruned by using the Optimal Brain Surgeon algorithm (Hassibi and Stork 1993) with regularization (Pedersen et al. 1995) until the best performance has been achieved. Initially, networks had 60 neurons, and their number and the number of weights has been reduced through the pruning process. The UVI assessment model in this case consisted of an ANN system with four ANNs (one SOM ANN and three feed-forward ANNs, one used for each of the clusters). When the best models are obtained for each of the clusters from the training set, then it was possible to evaluate behavior on the test set. When data is presented to the ANN system, firstly SOM ANN determines which of the three clusters the data belongs to, and then the feed-forward ANN for that cluster makes prediction of the UVI. The number of data found in the test set in different clusters is given in Table 6.2.

6.5 Results for the Second Model

The results for this model are captured in Figures 6-7 to Fig. 6-10 for the initial results. One notices that the results in this case appear to be something better on the test set than on the training set. The reason may be that, although the separation of the data to the training and test set is made by random selection of locations, the training set may happen to contain more diversified data in clusters than the clusters in the test set. However, the distribution of the cumulative errors on both training and test sets are better for the second model than for the first model

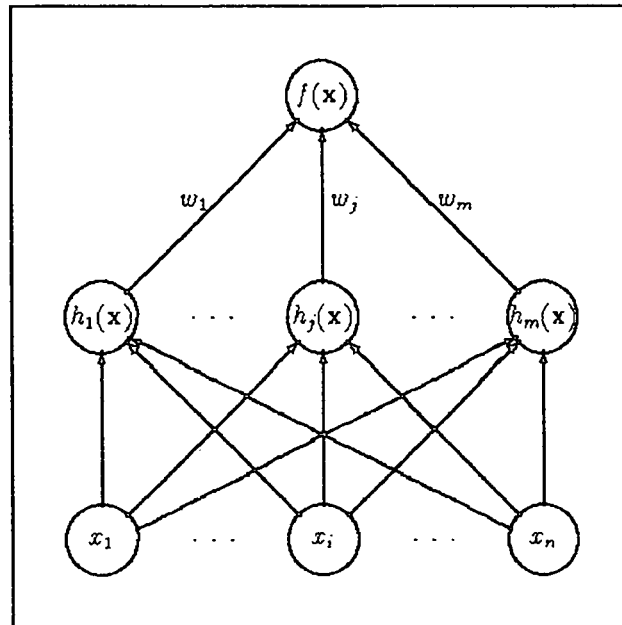


Figure 6-6: Simplified structure of a three layered feed-forward neural network. In our case the output neurons are linear, while the hidden layer neurons are of 'tansig' type, thus having $h_j(x) = \frac{e^x - e^{-x}}{e^x + e^{-x}}$. The initial number of neurons in the hidden layer was 60, and through the pruning process it has been reduced so as that the prediction performance of the neural network model has improved.

on the test set. This is important, since this illustrates the generalization properties of the second model. For this model, notice that for more than 91% of data in the training set and more than 96% of data in the test set, the maximum prediction error is ± 3 . However, for the first model, 98% of data from the training set makes maximum prediction error ± 3 , while its performance on the test set deteriorates considerably making such errors only for 82% of cases. This is good indication that the first model cannot generalize well. In any case, the results indicate that the second model generalizes well, which means that clustering of the data was justified.

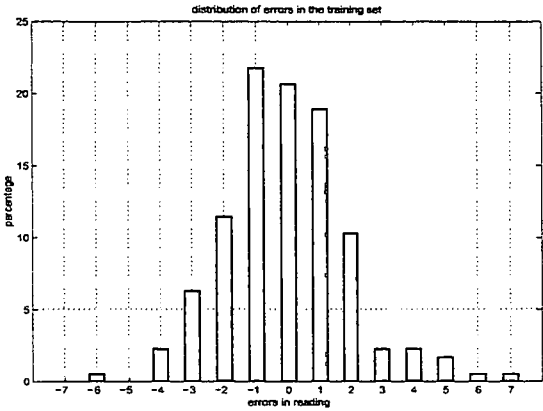


Figure 6-7: Distribution of prediction errors in the training set with the improved model.

6.5.1 Reduction of data - a way to improve the model

It was noticed that there is a small number of outliers in the datasets. When 18 outliers were removed from the datasets, and the system retrained in the same way as it was done for the second model, the maximum error (on both training and test sets) was ± 3 units in the 0 – 15 scale for the UVI. The distributions of error are captured in Fig. 6-11 to Fig. 6-14. Note that 18 outliers represent only 6.62% of the whole dataset. Thus by a small reduction of the number of the original data, the precision of the model considerably increased.

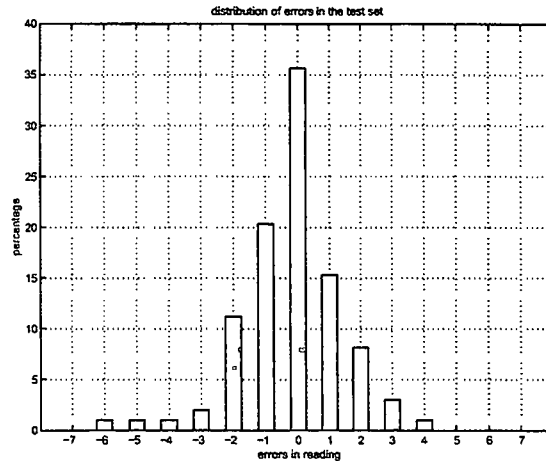


Figure 6-8: Distribution of prediction errors in the test set with the improved model.

By eliminating in total 38 outliers, which represent 13.97% of the whole dataset, the maximum error of the retrained model reduces now to ± 2 . The distributions of errors for training and test sets are given in Fig. 6-15 to Fig. 6-18. The same comments as in the previous case hold.

As can be concluded, we found that clustering of data allows for the generation of good quality models for UVI predictions. The model handled relatively easily the fuzziness in the data and the categorical nature of some of the variables. We also noticed that pruning of the ANN models tends to make robust models with good generalization abilities. Reduction of data also improved the precision of the models to some extent.

6.6 Third Model

Encouraged by the results of the previous section, we attempted to generate a different model by using more clusters. However, as the number of data available for this research was collected from a relatively modest number of sites, we selected this

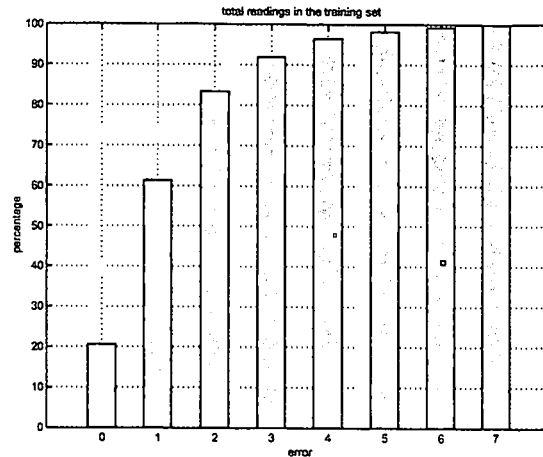


Figure 6-9: Distribution of cumulative prediction errors in the training set with the second model.

time to have only four clusters. A SOM ANN was used again, as in the previous section. The SOM ANN was trained in 200,000 epochs. For each of the clusters, we now used an RBNN and trained it to make an assessment of the UVI from the data in the cluster. Again, the training was done by using data from the relevant clusters of the training set, while testing is made on the respective clusters of the test set. Training of the individual RBNNs is done in the same way as in the section describing the first ANN model.

The ANN system now had five ANNs: one SOM and four RBNNs. The final results on the test set are depicted in Fig. 6-19 and Fig. 6-20. This model seems to produce the results similar to those of the second model. However, it produces most of the correct predictions from all models. For example, in about 40% of the cases there was **no error** in assessment of the UVI. Note that this was not possible to achieve with any of the previous models.

As a conclusion, these results evidently demonstrate the ability to relatively accurately predict the UVI from the collected data. This also emphasize the relevance of the selected variable in description of the UVI model. The results obtained with

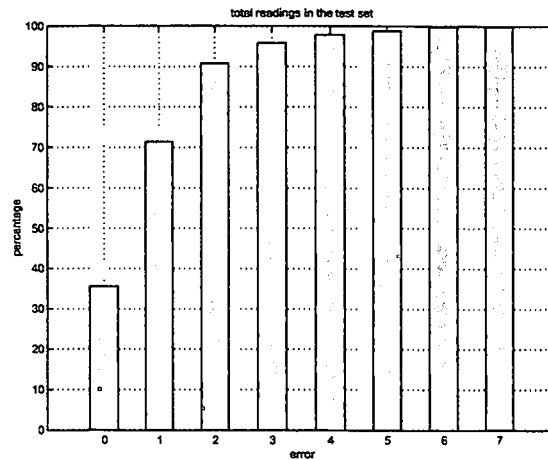


Figure 6-10: Distribution of cumulative prediction errors in the test set with the second model.

the second and the third model are at the level of accuracy achieved by the much more sophisticated and considerably more expansive system used in Canada for UVI forecast (Long 1997).

There is a possibility to further improve these results. The available data set is relatively small, so that by making more extensive coverage of the South African territory in the solar survey could enrich the data set to enable more effective and more accurate training of the ANN systems. Another problem, that cannot be resolved is the imprecision inherent in some of the basic input data. This would remain as a problem, but we see that the ANN systems do handle these effectively.

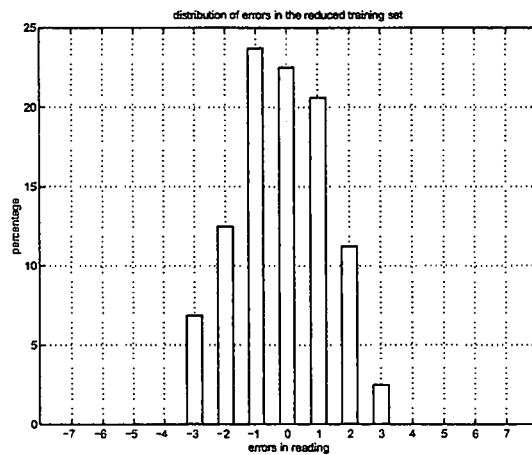


Figure 6-11: Distribution of prediction errors in the first reduced training set with the second model.

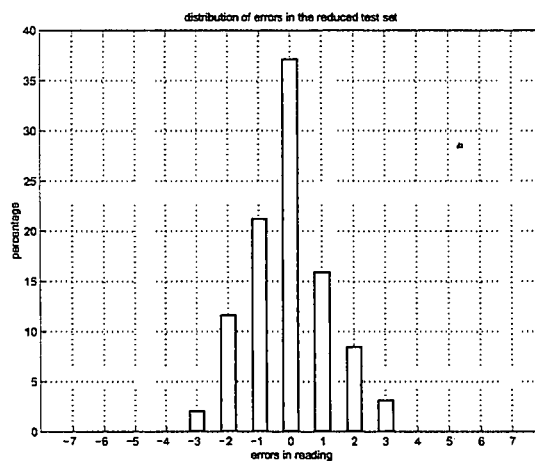


Figure 6-12: Distribution of prediction errors in the first reduced test set with the second model.

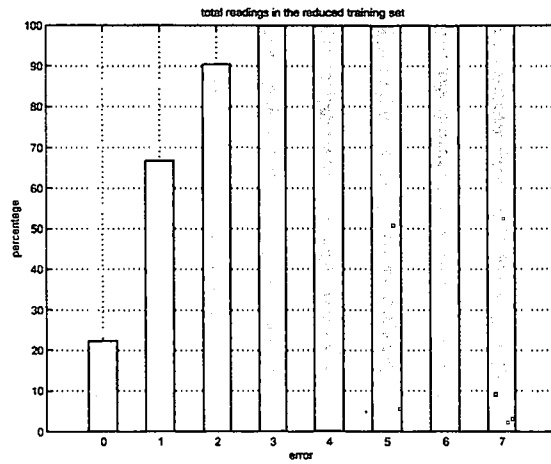


Figure 6-13: Distribution of cumulative prediction errors in the first reduced training set with the improved model.

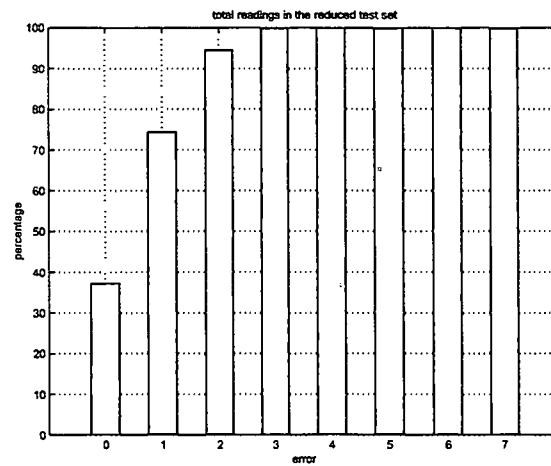


Figure 6-14: Distribution of cumulative prediction errors in the first reduced test set with the improved model.

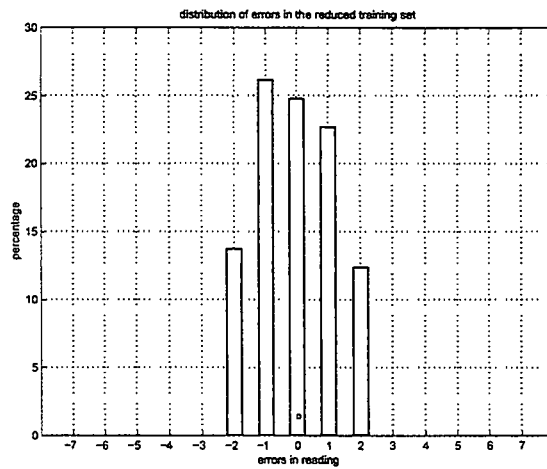


Figure 6-15: Distribution of prediction errors in the second reduced training set with the second model.

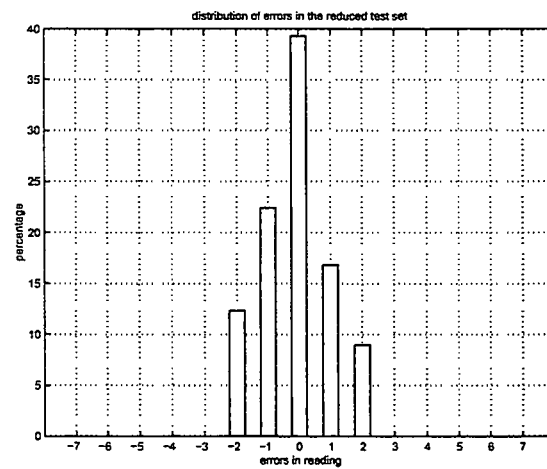


Figure 6-16: Distribution of prediction errors in the second reduced test set with the second model.

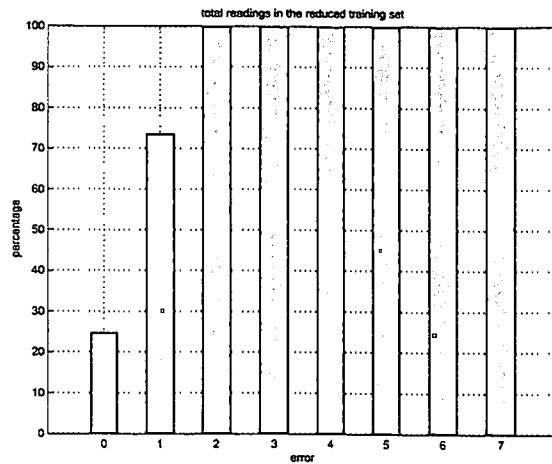


Figure 6-17: Distribution of cumulative prediction errors in the second reduced training set with the improved model.

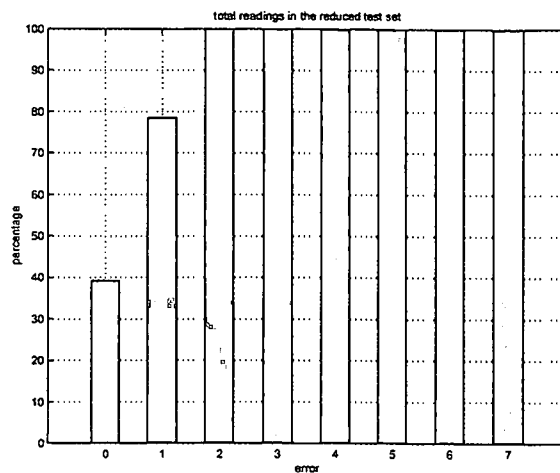


Figure 6-18: Distribution of cumulative prediction errors in the second reduced test set with the improved model.

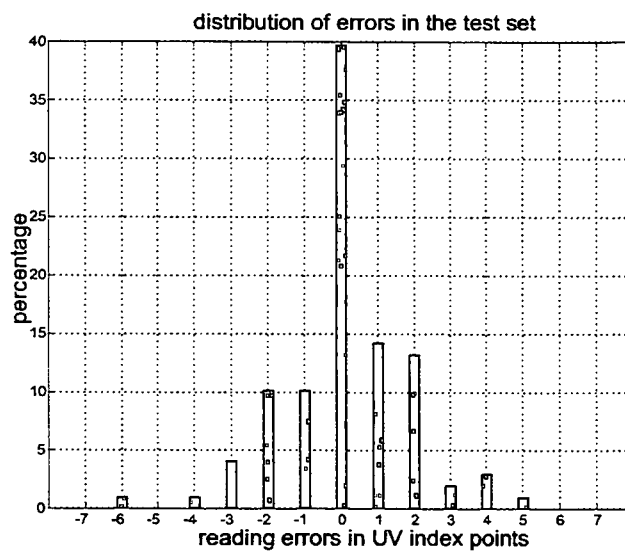


Figure 6-19: Distribution of predictive errors on the test set for the third model.

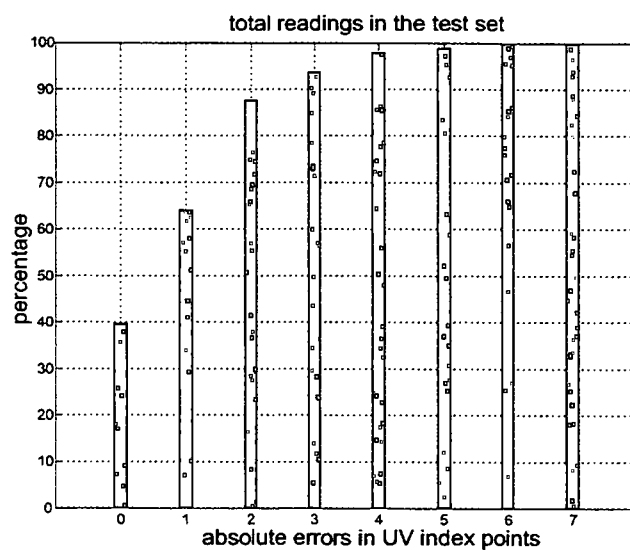


Figure 6-20: Cumulative error distribution for the third model on the test set given in %.

Chapter 7

Conclusions

This research developed several ANN based models aimed to predict the UVI from imprecise and fuzzy data (Viertl 1996) gathered in the only South African solar survey. The models obtained have been shown to have very good accuracy. The ANN based UVI models have much greater accuracy than that obtained by the classical regression (linear and nonlinear) techniques. Although we used only three types of ANNs in our modelling efforts (SOM, RBNN and feedforward), the evaluation of other network structures could provide possibly better results. The same holds true regarding different ANN training algorithms.

It was found that it makes sense to cluster data to smaller groups to increase the overall model accuracies (second and third ANN models). This inevitably required much more data than initially gathered in order to have ANNs involved well trained. However, even with the available modest dataset we were able to produce excellent results, with accuracy of the UVI prediction higher than that obtained with much more complex and expensive systems (Long 1997). This shows that the approach adopted was good.

One of the problems experienced was associated with the imprecise and fuzzy nature of a part of the data. We noticed that ANNs do handle this relatively easy, while the standard regression techniques did not cope well. The reason probably is that the more complex structure of the ANN based models used in this research,

allows for the suitable adjustment of model parameters so as to make the regression problem easier when utilizing ANNs.

Another of the problems experienced is the relatively small number of locations (272) from which data has been collected. With the more comprehensive dataset the ANNs would be better trained and chances that the model will achieve greater accuracy are much higher. Also, coastal regions could be covered by more dense location network. Consequently, further attempts must be made to repeat such a solar survey in a much broader scope and to include UVA irradiances as well. This will yield the UVA_{max} for South Africa during such a survey, and may prove very useful in deciding what UVA protection broad spectrum sunscreens should provide.

The results achieved in this research show that it is possible to infer accurate UVI from data that are easily available across the country. This is necessary in order to establish a nationwide network that will provide information to general population to appreciate the danger to the human body due to prolonged UV exposure. An almost nationwide understanding of the health risks due to high UVI is necessary if the UVI related health problems are to be reduced in all population groups in the long term. In particular, all awareness drives, including educational and dissemination programmes can and should be based on the UVI. In the Southern Hemisphere the Australian 'SunSmart' programme has been in place for twenty years and only now do statistics prove a reduction in some skin cancer figures. This typical time lag in being able to actually observe the difference in health statistics **MUST** surely serve as a warning to South Africa.

We in **South Africa**, with no coordinated National programme in place, will have to **wake up** if we wish to address such diverse issues as the Gross National Product (GNP), the taxpayer, and relevant medical services to cope with **skin cancer** and eye disorders caused by UVR. Efforts must immediately be made to reach members of our population, especially children, scholars and active people, so that we can combat these UVR related health problems with knowledge of its causes, and that a core of informed South Africans emerges **as soon as possible**. **UVI**

maps of South Africa should be made available on a daily basis, via all written and electronic media. Furthermore, forecasts giving predictions for the following day, will ensure that we all are prepared against overexposure by **taking** the necessary **precautions**.

Chapter 8

Bibliography

- ARPANSA (1999) *Resource Guide for UVR Protective Products*.
- Bajic V. B. and Human S. (1999) Estimation of UV Index Value by Neural Networks, in *Development and Practice of Artificial Intelligence Techniques*, 75–77
- Burrows W. R. (1997) Cart Regression Models for Predicting UV Radiation at the Ground in the Presence of Cloud and Other Environmental Factors, *Journal of Applied Meteorology* **36**(5):531–544
- Cesarini J. P. (1998a) Ultraviolet Action Spectra for Photosensitization. *Measurements of Optical Radiation Hazards*, 81–91
- Cesarini J. P. (1998b) CIE Efforts in Standardization of Action Spectra. *Measurements of Optical Radiation Hazards*:233–237
- Cesarini J. P. (2000) Toward a Genotoxic Protection Factor. *Radiation Protection Dosimetry* **91**(1–3):89–91
- Cesarini P. (1998) UV Index and Communicating UV Information to the Public. *Measurements of Optical Radiation Hazards*, 437–442
- Cesarini P. (2000) UV Indices, Durban. E-mail/Meteoconsult private communication.

- CIE Research Note (1987) A Reference Action Spectrum for Ultraviolet Induced Erythema in Human Skin, *CIE-Journal* 6(1)17-22
- Cullen A. P. (1998) The Lens -Ultraviolet and Infrared Action Spectra for Cataract Acute In Vivo Studies. *Measurements of Optical Radiation Hazards*, 159-171
- de Gruijl F. R. (2000) Biological Action Spectra. *Radiation Protection Dosimetry* 91(1-3):57-63
- DeLuisi J., Augustine J., Theisen D., Weatherhead E., Disterhoft P., Lantz K. and Herman J. (1998) Solar UV Monitoring Network Operations and Data Quality Assurance with TOMS Observations. *Measurements of Optical Radiation Hazards*, 603-617
- Diffey B. L. (1989) A new substrate to measure sunscreen protection factors throughout the ultraviolet spectrum. *Journal of the Society of Cosmetic Chemists* 40:127-133
- Diffey B. L. (1992) Sun Protection with Hats. *British Journal of Dermatology* 127:10-12
- Diffey B. L. (1998) The confounding influence of sun exposure in melanoma, *The Lancet* 351:1101-1102
- Diffey B. L. (2000) Personal Protection: The Way Forward. *Radiation Protection Dosimetry* 91(1-3):293-296
- Diffey B. L. (1999) Diffey Erythema Spectrum: Graphs relating Power/m² and wavelength showing three ozone densities, Safesun, 13
- Dransfield G. P. (2000) Inorganic Sunscreens. *Radiation Protection Dosimetry* 91(1-3):271-273
- Gies H. P. (1990) A proposed UVR protection factor for sunglasses, *Clinical & Experimental Optometry* 73(6):184-189

- Gies H. P. (1992) Ultraviolet Radiation Protection Factors for Clear and Tinted Automobile Windscreens. *Radiation Protection in Australia* **10**(4):91-94
- Gies H. P. (1992) Ultraviolet Radiation Protection Factors for Personal Protection in Both Occupational and Recreational Situations. *Radiation Protection in Australia* **10** (3):59-65
- Gies H. P. (1994) The ARL solar UVR measurement network: Calibration and results. *SPIE Ultraviolet Technology* **2282**:274-283
- Gies H. P. (1994) Ultraviolet Radiation Protection Factors for Clothing. *Health Physics* **67**(2):131-137
- Gies H. P. et al. (1997) Protection against solar radiation, *Mutation Research*, **422**, 15-22
- Gies H. P. (1997) UV Protection by Clothing: An Intercomparison of Measurements and Methods, *Health Physics* **73**(3):456-464
- Gies H. P. (1998) Solar UVR Exposures of Primary School Children at Three Locations in Queensland, *Photochemistry and Photobiology* **68**(1):78-83
- Gies P. H. (1998) Protection against solar ultraviolet radiation, *Mutation Research* **422**:15-22
- Gies P. H. (1999) Ambient Solar UVR, Personal Exposure and Protection. *Journal of Epidemiology*, **9**(6):115-122
- Hassibi B. and Stork G. D. (1993) Second order derivatives for network pruning: Optimal Brain Surgeon, *NIPS 5*, Eds. S. J. Hanson et al., 164, San Mateo, Morgan Kaufmann.
- Hawk J. L. M. (2000) Sunbeds. *Radiation Protection Dosimetry* **91**(1-3):143-145
- Hilfiker R. (1989) Determination of Sun Protection Factors (SPF) of Fabrics at CIBA. Ciba Research Services, *PHYSICS*:1-3

- Holick M. F. (2000) Sunlight and Vitamin D: The Bone and Cancer Connections. *Radiation Protection Dosimetry* **91**(1-3):65-71
- Hopkins R. (2000) UV Index Categories, private communication.
- Human S. and Bajic V. (2000) Modelling Ultraviolet Irradiance in South Africa. *Radiation Protection Dosimetry* **91**(1-3):181-183.
- Human S. (2000) Contribution to Skin Cancer Prevention in South Africa: Modelling the UV Index utilising imprecise data. International Data Analysis Conference, Innsbruck, Austria
- IRPA/INIRIC Guidelines (1989) Proposed Change to the IRPA 1985 Guidelines on Limits of Exposure to Ultraviolet Radiation. *Health Physics* **56**(6):971-972
- Kok C. J. (1979) Spectroradiometry of daylight at sea level in the Southern Hemisphere: Durban. *South African Journal of Physics* **2**(2):47-53
- Long J. (1997) Monitoring UV, *Proc. of the Skin Cancer Conference*, Les Diablerets, Switzerland, 45-62.
- Lowe N. J. (1995) UV Protection offered by clothing: An *in vitro* and *in vivo* assessment of summer clothing fabrics. *Skin Cancer* **10**:89-96
- Lowe A. J. and O'Hagan J. B. (2000) The Safe Use of Ultraviolet Lasers in Industry and Research. *Radiation Protection Dosimetry* **91**(1-3):223-226
- Lubin D. (1998) Global surface ultraviolet radiation climatology from TOMS and ERBE data, *Journal of Geophysical Research*, **103**:D20:26061- 26091
- Jonker D. L. (1994) UV-Induced Skin Darkening in Negroid Skin. *Cosmetics & Toiletries* **109**:51-58
- Mackie R. M. (2000) Effects of Ultraviolet Radiation on Human Health. *Radiation Protection Dosimetry* **91**(1-3):15-18

- Marks R. (1993) Trends in non-melanocytic skin cancer treated in Australia: The Second National Survey. *International Journal of Cancer* **53**:585–590
- Mellerio J. (1998) The Design of Effective Ocular Protection for Solar Radiation. *Measurements of Optical Radiation Hazards*, 323–340
- Menter J. M. (1994) Protection against UV photocarcinogenesis by fabric materials. *Journal of the American Academy of Dermatology* **31**:711–716
- Moise A. F. (1999) Solar ultraviolet exposure of infants and small children, *Photo-dermatol. Photoimmunol. Photomed.* **15**:109–114, ISSN 0905–4383
- Moon R. (1995) Effect of Stretch and Wetting on the UPF of Elastane Fabrics. *Australasian Textiles*, 39–41
- NASA (1997) Action Spectra. Stratospheric Ozone and Human Health Project.
- Nelder J. A. and Mead R. (1965) A Simplex Method for Function Minimization, *Computer Journal*, **7**:308–313.
- Norval M. (2000) The Impact of Ultraviolet Radiation on Immune Responses. *Radiation Protection Dosimetry* **91**(1–3):51–56
- NRPB (1995) Board Statement on Effects of Ultraviolet Radiation on Human Health and Health Effects from Ultraviolet Radiation. *Documents of the NRPB* **6** (2):Fig 6.3– Fig 6.12
- O’Riordan D. L. (2000) Correlations between Reported and Measured Ultraviolet Radiation Exposure of Mothers and Young Children, *Photochemistry and Photobiology* **71**(1):60–64
- Orr M. (1999) Recent Advances in Radial Basis Function Networks, Technical Report, <http://www.anc.ed.ac.uk/~mjo/rbf.html>.

- Osterwalder U., Schlenker W., Rohwer H., Martin E. and Schuh S. (2000) Facts and Fiction on Ultraviolet Protection by Clothing. *Radiation Protection Dosimetry* 91(1-3):255- 260
- Pederson M. W., Hansen L. K. and Larsen J. (1995) Pruning with generalization based weight saliences, *Proc. of the Neural Information Processing Systems*, 8.
- Peeters P., Simon P. C., Hansen G., Meerkoetter R., Verdebout J., Seckmeyer G., Taalas P. and Slaper H. (2000) MAUVE: A European Initiative for Developing and Improving Satellite Derived Ultraviolet Maps. *Radiation Protection Dosimetry* 91(1-3):201-202
- Pham D. T. (1995) *Neural Networks for Identification, Prediction and Control*, 1-60
- Rengarajan G., Weihs P., Simic S., Mikieliewicz W. and Laube W. (2000) Albedo Measurement System for UVA and the Visible Wavelength. *Radiation Protection Dosimetry* 91(1-3):197-199
- Rosner B. (1990) *Fundamentals of biostatistics*, PWS-Kent, Boston.
- Roy C. R. et al (1997) The measurement of solar ultraviolet radiation, *Mutation Research*, 422:7-14
- Sasaki K. (1998) The Lens - Human Data from Chronic Exposure: UV Related Cataract. *Measurements of Optical Radiation Hazards*, 179-192
- Sayre R. M. (1993) Sun Protective Apparel:Advancements in Sun Protection. *Skin Cancer* 8:41-47
- Sinclair C., Dobbinson S. and Montague M. (2000) Can a Skin Cancer Programme make a Difference? A Profile of the SunSmart Programme in Victoria. *Radiation Protection Dosimetry* 91(1-3):301-302

- Sitas F., Madhoo J. and Wessie J. (1998) *Cancer in South Africa 1993-1995*.
- Skin Factors (1999) Safesun Threshold Doses for Different Skin Types, 16
- Sliney D. H. (1987) Transmission of potentially hazardous actinic ultraviolet radiation through fabrics. *Applied Industrial Hygiene* 2:36-44
- Sliney D. (1998) Photobiological Action Spectra -What do they mean? *Measurements of Optical Radiation Hazards*, 41-47
- Sliney D. H. and Bitran M. (1998) The ACGIH Action Spectra for Hazard Assessment: The TLV's. *Measurements of Optical Radiation Hazards*, 241-259
- Stanford D. G. (1995) Sun protection by a summer-weight garment:the effect of washing and wearing. *The Medical Journal of Australia* 162:422-425
- Stanford D. G. (1995) The effect of laundering on the sun protection afforded by a summer weight garment. *Journal of the European Academy of Dermatology and Venereology* 5:28-30
- Summers B. (1999) *The Millenium Sunscreen Update*, 1-6
- Toomey S. J. (1995) UVR Protection offered by Shadecloths and Polycarbonates, *Radiation Protection in Australia*, 13(2):50-54
- UV NET Database (1998) CIE, ICNIRP & ACGIH UV-hazard action spectrum, 250-400 nm
- Viertl R. (1996) *Statistical Methods for Non-Precise Data*, 1-69, CRC-Press.
- van Tonder N. (1998) Protective Qualities of UV Shading Materials. *Measurements of Optical Radiation Hazards*, 429-436
- Webb A. R. (2000) Standardisation of Data from Ultraviolet Radiation Detectors. *Radiation Protection Dosimetry* 91(1-3):123-128

- Weihs P., Rengarajan G., Simic S., Laube W. and Mikielwicz W. (2000) Measurements of the Reflectivity in the Ultraviolet and Visible Wavelength Range in a Mountainous Region. *Radiation Protection Dosimetry* **91**(1-3):193-195
- Wester U. (2000) Measurements of Solar UVA, UVB and Ozone: Estimates of Population Ultraviolet Doses. *Radiation Protection Dosimetry* **91**(1-3):115-118
- WHO/EHG/ (1995) 95.16. *Health and Environmental Effects of Ultraviolet Radiation*, 3-21
- WHO FACT SHEET (1999) Solar Radiation and Human Health # 227, 3rd Aug.
- Wilkinson F. (1998) Solar Simulators for Sunscreen Testing. *Measurements of Optical Radiation Hazards: 653-684*.
- Zurada J. M. (1992) *Introduction to Artificial Neural Systems*, West Publishing Company, St.Paul, Minnesota